fractal and fractional

MDPI

Article

Observer-Based Prescribed Performance Adaptive Neural Network Tracking Control for Fractional-Order Nonlinear Multiple-Input Multiple-Output Systems Under Asymmetric Full-State Constraints

Shuai Lu *, Tao Yu and Changhui Wang *

School of Electromechanical and Automotive Engineering, Yantai University, 32 Qingquan Road, Laishan District, Yantai 264005, China; yt_126@126.com

* Correspondence: lushuai405@163.com (S.L.); wang_changhui@126.com (C.W.)

Abstract: In this work, the practical prescribed performance tracking issue for a class of fractional-order nonlinear multiple-input multiple-output (MIMO) systems with asymmetric full-state constraints and unmeasurable system states is investigated. A neural network (NN) nonlinear state observer is developed to estimate the unmeasurable states. Furthermore, the barrier Lyapunov functions with the settling time regulator are employed to deal with the asymmetric full-state constraint from the fractional-order MIMO system. On this ground, the prescribed performance adaptive tracking control approach is designed, assuring that all system states do not exceed the prescribed boundaries, and the tracking errors converge to the predetermined compact sets within a predefined time. Finally, two simulation examples are presented to show the effectiveness and practicability of the proposed control scheme.

Keywords: fractional-order systems; MIMO; asymmetric full-state constraints; prescribed performance; predefined time

Citation: Lu, S.; Yu, T.; Wang, C. Observer-Based Prescribed Performance Adaptive Neural Network Tracking Control for Fractional-Order Nonlinear Multiple-Input Multiple-Output Systems Under Asymmetric Full-State Constraints. *Fractal Fract.* **2024**, *8*, 662. https://doi.org/10.3390/fractalfract8110662

Academic Editor: David Kubanek

Received: 5 October 2024
Revised: 27 October 2024
Accepted: 1 November 2024
Published: 13 November 2024

1. Introduction

In the past few decades, the nonlinear systems control issue with uncertainty has become a hot topic. At present, a lot of controller methods have been designed, in which the backstepping scheme is an effective way for the nonlinear control system [1–5]. However, for parameterization or for when the structure of the nonlinear system is not linear, the limitations of the backstepping method become apparent, especially when the nonlinear systems are more complex. To overcome this shortcoming, the advanced intelligent algorithms have been used as the main tool, in which the fuzzy logic systems (FLSs) and neural networks (NNs) are employed to construct the nonlinear uncertain structures [6–9]. The authors in [6] design a robust adaptive fuzzy control scheme for the second-order Euler–Lagrange systems, and the authors in [7] investigate the tracking control issue for the time-varying pure-feedback system, in which the nonlinearities are approximated by FLSs. The authors in [8] study an adaptive NN control method for the uncertain flexible manipulator, and the authors in [9] propose an adaptive NN tracking controller for underwater vehicles in which the NNs are applied to approximate the system uncertainty.

In many engineering applications, there are lots of constraints in the actual systems, such as the fact that the system states can only change within the fixed physical ranges, and the system may be unstable when the state constraints are violated. For instance, trajectory tracking control for underwater vehicles was developed in [10], in which the state constraints are handled by the transformation functions. In [11], the tracking controller for firefighting robots with full-state constraints was designed, in which the state-dependent transformation function was present to address the state constraints. In [12], a two-layer control scheme was developed for the linear motors with state constraints, in which a

time-optimal controller was considered as the upper layer and a robust controller was used as the lower layer. In [13], an adaptive controller for cable tower cranes system with state constraints is designed, in which the state constraints are from the safety and transportation requirements. In [14], an adaptive controller with guidance is presented for the ascent hypersonic vehicle under multiple state constraints, in which the barrier Lyapunov function (BLF) is used to address the conditions.

The rapid convergence of the closed-loop system may lead to excessive overshoot, making it difficult to obtain the necessary tracking accuracy, which are the basic goals in the nonlinear system tracking control. The prescribed performance control scheme can ensure the tracking errors stay in predefined bounds to improve the transient and steady-state performance. In [15], an adaptive tracking controller with performance optimization is designed for nonlinear system to guarantee the prescribed performance. In [16], a prescribed performance tracking controller for strict-feedback nonlinear system is presented, in which the barrier error transformations is employed. In [17], a global prescribed performance adaptive control method using backstepping framework is designed for the Markov jumping system. In [18], a prescribed performance adaptive fuzzy control scheme for a robot system was developed by using the disturbance observer and auxiliary system. In [19], a prescribed performance optimal adaptive controller for autonomous vehicles was designed, in which a prescribed performance function with dynamic programming was introduced to constrain the tracking errors.

Fractional-order calculus, as an extension of integral-order calculus, can accurately describe many physical systems on account of the infinite memory. As a result, fractional-order systems show great potential in a variety of areas, such as biological systems [20–22], viscoelastic materials [23–25], power systems [26–28], financial fields [29,30], and so on. However, it is worth mentioning that many of the above practical fractional-order systems are multiple-input multiple-output (MIMO) nonlinear uncertainty systems. In [31], an adaptive fuzzy controller based on a fuzzy state observer was designed for the fractional-order uncertain MIMO nonlinear system to ensure the boundedness of all signals. In [32], a switched adaptive controller for a fractional-order MIMO system was presented in which the derivation order can be switched between the integer order and fractional order. In [33], a state observer based on modulating function was designed for an integer and fractional-order MIMO system, which can estimate both the states and fractional derivatives simultaneously. In [34], the adaptive fuzzy control method for fractional-order MIMO system with state constraints was presented in which the BLF was presented for the states meeting the specified limits. In [35], a novel approach for a fractional-order MIMO system to generate a low dimension state-space model was proposed, and the realization condition for state-space model was presented. However, as far as the author knows, the prescribed performance tracking control schemes for a fractional-order nonlinear MIMO system with asymmetric full-state constraints and unmeasurable system states have been hardly investigated, which will be a meaningful and challenging work.

Inspired by the above discussions, a practical prescribed performance tracking control strategy based on a nonlinear state observer for constrained fractional-order nonlinear MIMO system is presented to guarantee the tracking performance. The significant contributions are listed as follows:

(1) Different from the existing BLF method in [34], the symmetric full-state constraints and prescribed performance are both considered here, and the non-piecewise BLF is presented to deal with the asymmetric state constraints, which is convenient to design a unified control strategy to handle asymmetric or symmetric full-state constraints.
(2) Comparing with the results on the finite-time controller for fractional-order systems [36,37], the tracking error can converge to a predetermined compact set in a preset time, and the convergence accuracy and setting time do not depend on the control parameters. The proposed scheme can make the tracking errors converge to the predetermined compact sets in a predefined time, in which the tracking performance and settling time are dependent of the adjustable parameters.

(3) Comparing with the results on the prescribed time controller for the integer order system in [38–40], the prescribed time control scheme for the more general constrained fractional-order nonlinear MIMO systems is designed, in which external disturbances are considered and unmeasurable states are estimated by the NN nonlinear observer, and the tracking performance and stability of the fractional-order closed-loop system in the specified time can be guaranteed.

2. Preliminaries

Definition 1 ([41]). *The fractional-order integral for $r(t) \in C^n([t_0, +\infty))$ is defined as:*

$$ {}_{t_0}^{C}\mathcal{D}_t^{-\alpha} r(t) = \frac{1}{\Gamma(\alpha)} \int_{t_0}^{t} r(\tau)(t-\tau)^{\alpha-1} \, \mathrm{d}\tau \tag{1} $$

where $\alpha \geq 0$, $t \geq t_0$ and $\Gamma(\alpha) = \int_0^{+\infty} s^{\alpha-1} e^{-s} ds$.

Definition 2 ([42]). *The Caputo's fractional-order derivative for $f(t) \in C^n([t_0, +\infty))$ is defined as:*

$$ {}_{t_0}^{C}\mathcal{D}_t^{\alpha} f(t) = \frac{1}{\Gamma(1-\alpha)} \int_{t_0}^{t} \frac{f'(\tau)}{(t-\tau)^{\alpha}} \mathrm{d}\tau \tag{2} $$

where $\alpha \in (0,1)$ and $t \geq t_0$. The Laplace transform of ${}_{t_0}^{C}\mathcal{D}_t^{\alpha} f(t)$ is defined as:

$$ \mathcal{L}\left\{ {}_{t_0}^{C}\mathcal{D}_t^{\alpha} f(t) \right\} = s^{\alpha} F(s) - s^{\alpha-1} F(0) \tag{3} $$

where $\mathcal{L}\{\cdot\}$ is the Laplace transform operator, and $F(s) = \mathcal{L}\{f(t)\}$.

Lemma 1 ([43]). *For functions $f_1(t)$ and $f_2(t)$, one can obtain:*

$$ \begin{array}{l} {}_{t}^{C}\mathcal{D}_b^{\alpha} f(t) = {}_{t}^{R}\mathcal{D}_b^{\alpha} + \frac{f(b)}{\Gamma(1-\alpha)}(b-t)^{-\alpha} \\ {}_{t}^{R}\mathcal{D}_b^{\alpha}(b-t)^{m} = -\frac{\Gamma(m+1)}{\Gamma(m-\alpha+1)}(b-t)^{m-\alpha} \end{array} $$

where $0 < \alpha < 1$, $b > t$, $m > 1$ and ${}_{t}^{R}\mathcal{D}_b^{\alpha} = -\frac{1}{\Gamma(1-\alpha)} \frac{d}{dt} \int_t^b \frac{f(\tau)}{(t-\tau)^{\alpha}} \mathrm{d}\tau$. ${}_{t_0}^{C}\mathcal{D}_t^{\alpha}$ can be simplified as $\mathcal{D}^{\alpha}$.

Lemma 2 ([44]). *For smooth function $f(x) : R^n \to R$ with $x = (x_1, \ldots, x_n) \in \Omega_x \subset R^n$ and compact set Ω_x, if the following Hessian*

$$ H(f(\cdot)) = \begin{pmatrix} \frac{\partial^2 f(x)}{\partial x_1^2} & \frac{\partial^2 f(x)}{\partial x_1 \partial x_2} & \cdots & \frac{\partial^2 f(x)}{\partial x_1 \partial x_n} \\ \frac{\partial^2 f(x)}{\partial x_2 \partial x_1} & \frac{\partial^2 f(x)}{\partial x_2^2} & \cdots & \frac{\partial^2 f(x)}{\partial x_2 \partial x_n} \\ \vdots & \vdots & & \vdots \\ \frac{\partial^2 f(x)}{\partial x_n \partial x_1} & \frac{\partial^2 f(x)}{\partial x_n \partial x_2} & \cdots & \frac{\partial^2 f(x)}{\partial x_n^2} \end{pmatrix} $$

is positive semi-definite, one can obtain $\mathcal{D}^{\alpha} f(x) \leq \sum_{i=1}^{n} \frac{\partial f(x)}{\partial x_i} \mathcal{D}^{\alpha} x_i$ for $\forall t \geq 0$ and $0 < \alpha < 1$.

Lemma 3. *For the continuously differentiable functions $f_1(t) \in R$ and $f_2(t) \in R_+^*$, the following inequality holds:*

$$ \mathcal{D}^{\alpha} \frac{f_1^2(t)}{f_2(t)} \leq 2 \frac{f_1(t)}{f_2(t)} \mathcal{D}^{\alpha} f_1(t) - \frac{f_1^2(t)}{f_2(t)} \mathcal{D}^{\alpha} f_2(t) \tag{4} $$

where $0 < \alpha < 1$, $t \geq 0$ and R_+^* is the set of positive real numbers.

Definition 3 ([45]). *The Mittag–Leffler function can be defined as:*

$$E_{a_1,a_2}(\delta) = \sum_{k=0}^{+\infty} \frac{\delta^k}{\Gamma(a_1 k + a_2)} \tag{5}$$

where $a_1, a_2 > 0$, δ *is a complex number. Then, the Laplace transform is:*

$$\mathcal{L}\left\{ t^{a_2-1} E_{a_1,a_2}(-ct^{a_1}) \right\} = \frac{s^{a_1-a_2}}{s^{a_1}+c}, \mathrm{Re}(s) > |c|^{\frac{1}{a_1}} \tag{6}$$

where $t \geq 0$, $a_1, a_2 > 0$, $c \in R$.

Lemma 4. *For* $0 < a < 1$, $c > 0$ *and* $t \geq 0$, *one can obtain:*

$$\begin{array}{l} 0 < E_{a,1}(-ct^a) \leq 1; E_{a,1}(-ct^a) \to 0 \quad \text{as} \quad t \to \infty; \\ 0 < E_{a,a}(-ct^a); 0 \leq t^a E_{a,a+1}(-ct^a) < \frac{1}{c} \end{array} \tag{7}$$

According to [46], a settling time regulator is defined as

$$\zeta(t) = \begin{cases} \left(\frac{T-t}{T}\right)^{2m}, & 0 \leq t \leq T \\ 0, & t > T \end{cases} \tag{8}$$

where $T > 0$, *and positive integer* m *satisfies* $2m > n+1$. *Then, a performance function can be defined as:*

$$\mathcal{P}(t) = \begin{cases} (1-k_a)\left(1-\frac{t}{T}\right)^{2m} + k_a, & 0 \leq t \leq T \\ k_a, & t > T \end{cases} \tag{9}$$

where $k_a \in (0,1)$.

3. System Description

Considering a fractional-order MIMO system as

$$\begin{array}{l} \mathcal{D}^{\alpha} x_{k,i_k} = h_{k,i_k} x_{k,i_k+1} + f_{k,i_k}\left(\overline{x}_{k,i_k}\right) + d_{k,i_k}(t), i_k = 1, \ldots, n_k - 1; k = 1, \ldots l \\ \mathcal{D}^{\alpha} x_{k,n_k} = h_{k,n_k} u_k + f_{k,n_k}(x) + d_{k,n_k}(t) \\ y_k = x_{k,1} \end{array} \tag{10}$$

where $x = \left(\overline{x}_{1,n_k}^T \quad \overline{x}_{2,n_k}^T \quad \ldots \quad \overline{x}_{l,n_k}^T\right)^T$ and $\overline{x}_{k,i_k} = \left(x_{1,i_k} \quad x_{2,i_k} \quad \ldots \quad x_{k,i_k}\right)^T \in \mathbb{R}^{i_k}$ are the state vectors, wherein all system signals except $x_{k,1}$ are immeasurable. $u_k \in R$ and $y_k \in R$ are the control input and the system output. $h_{k,i_k} > 0 \in R$ expresses the known constant. $f_{k,i_k} \in R$ stands for the unknown smooth nonlinear function. While $d_{k,i_k}(t)$ indicates the unknown bounded external disturbance, which satisfies $d_{k,i_k}(\cdot) \leq d_{k,i_k}^*$ with $d_{k,i_k}^* \geq 0$ being constant.

Remark 1. *It is worth mentioning that fractional-order calculus includes classical integer order calculus when the order is equal to 1. Fractional-order systems (10) can be used to describe lots of practical systems, such as robotic manipulators [47], mechanical systems [48], power systems [49,50], etc.*

Based on (8) and (9), the performance function can be constructed as:

$$\mathcal{P}_k(t) = \begin{cases} (1-k_a)\left(1-\frac{t}{T_k}\right)^{2m} + k_a, & 0 \leq t \leq T_k \\ k_a, & t > T_k \end{cases} \tag{11}$$

where $k_a \in (0,1)$, and the settling time regulator is

$$\zeta_k(t) = \begin{cases} \left(\frac{T_k - t}{T_k}\right)^{2m}, & 0 \le t \le T_k \\ 0, & t > T_k \end{cases} \tag{12}$$

According to $z_{k,1} = x_{k,1} - y_{k,d}$, the constraint on $x_{k,1}$ can be translated as $-\kappa_{k,1,1} < z_{k,1} < \kappa_{k,1,2}$, where $\kappa_{k,1,1}, \kappa_{k,1,2} > 0$. Then, both the practical prescribed time tracking and the preset constraints can be completed if the following inequalities are satisfied:

$$-\kappa_{k,11}\mathcal{P}_k(t) < z_{k,1} < \kappa_{k,1,2}\mathcal{P}_k(t) \tag{13}$$

Through selecting $k_a = \min\{\epsilon_k/\kappa_{k,1,1}, \epsilon_k/\kappa_{k,1,2}\} < 1$ with parameter ϵ_k, it yields $|z_{k,1}| < \epsilon_k$ for $t > T_k$ by using (13).

The foremost objective is to propose an adaptive control strategy so that the following purposes are satisfied:

The control objectives of this article are listed as follows:

(1) Design an adaptive control strategy to ensure the boundedness of all closed-loop system.
(2) Tracking error $z_{k,1}$ can converge to the preset set $\Omega_{z_{k,1}} = \{z_{k,1} \in R : |z_{k,1}| < \epsilon_{k,1}\}$.
(3) The system state satisfies the following bounded constraints

$$\begin{aligned} \mathfrak{D}_{x_{k,1}} &= \{ x_{k,1}(t) | y_{k,d} - \kappa_{k,1,1} < x_{k,1}(t) < y_{k,d} + \kappa_{k,1,2} \} \\ \mathfrak{D}_{x_{k,i_k}} &= \{ x_{k,i_k}(t) | -\kappa_{k,i_k,1} < x_{k,i_k}(t) < \kappa_{k,i_k,2}, i_k = 2, \ldots, n_k; k = 1, \ldots l \} \end{aligned}$$

where $\kappa_{k,i_k,1}, \kappa_{k,i_k,2} > 0$ and $x_{k,i_k}(0) \in \mathfrak{D}_{x_{k,i_k}}$.

Assumption 1. *The desired signals $y_{k,d}(t)$ and $\mathcal{D}^\alpha y_{k,d}(t)$ and $\mathcal{D}^\alpha(\mathcal{D}^\alpha y_{k,d})$ are continuous and bounded.*

Assumption 2. *The function $f_{k,i_k}(\cdot)$ is the Lipschitz function, that is, $|f_{k,i_k}(\overline{x}) - f_{k,i_k}(\overline{y})| \le c_{k,i_k}\|\overline{x} - \overline{y}\|$ is satisfied, where $\forall \overline{x}, \overline{y}, \exists c_{k,i_k} > 0$.*

Remark 2. *In this paper, Assumptions 1 and 2 are used to design the adaptive controller. Assumption 1 can ensure that the ideal trajectories are bounded and available, which is reasonable and non-conservative, since the desired trajectories in real systems are generally continuous and efficient. Assumption 2 is used to deal with the relationship between $f_{k,i_k}(\overline{x}_{k,i_k})$ and $f_{k,i_k}(\hat{\overline{x}}_{k,i_k})$, which will be applied to closed-loop system stability analysis.*

4. Neural Network State Observer Design

In this section, a fractional-order NN state observer will be presented to estimate the immeasurable system states, in which RBF NNs with the ability to approximate continuous functions are used to approximate the unknown function.

The unknown function $f_{k,i_k}(\hat{\overline{x}}_{k,i_k})$ is presented as [51]:

$$f_{k,i_k}(\hat{\overline{x}}_{k,i_k}) = \theta_{k,i_k}^T S_{k,i_k}(\hat{\overline{x}}_{k,i_k}) + \varepsilon_{k,i_k}(\hat{\overline{x}}_{k,i_k}), \quad |\varepsilon_{k,i_k}(\hat{\overline{x}}_{k,i_k})| \le \bar{\varepsilon}_{k,i_k} \tag{14}$$

where

$$\theta_{k,i_k} = \operatorname{argmin}_{\hat{\theta}_{k,i_k} \in \Omega_{k,i_k}} \sup_{\hat{\overline{x}}_{k,i_k} \in \Omega_{\hat{\overline{x}}_{k,i_k}}} \left| f_{k,i_k}(\hat{\overline{x}}_{k,i_k}) - \hat{\theta}_{k,i_k}^T S_{k,i_k}(\hat{\overline{x}}_{k,i_k}) \right| \tag{15}$$

and Ω_{k,i_k} and $\Omega_{\hat{\overline{x}}_{k,i_k}}$ are the compact sets, $S_{k,i_k}(\cdot)$ is the basis function.

Based on (10), one can obtain

$$\begin{cases} \mathcal{D}^{\alpha} x_{k,i_k} = h_{k,i_k} x_{k,i_k+1} + \Delta f_{k,i_k}(\hat{\bar{x}}_{k,i_k}) + \theta_{k,i_k}^T S_{k,i_k}(\hat{\bar{x}}_{k,i_k}) + \Lambda_{k,i_k} \\ \mathcal{D}^{\alpha} x_{k,n_k} = h_{k,n_k} u_k + \Delta f_{k,n_k}(\hat{\bar{x}}_{k,n_k}) + \theta_{k,n_k}^T S_{k,n_k}(\hat{\bar{x}}_{k,n_k}) + \Lambda_{k,n_k} \end{cases} \tag{16}$$

where $\hat{\bar{x}}_{k,i_k}$ is the estimate value of state $\bar{x}_{k,i_k}$, $\Delta f_{k,i_k}(\hat{\bar{x}}_{k,i_k}) = f_{k,i_k}(\bar{x}_{k,i_k}) - f_{k,i_k}(\hat{\bar{x}}_{k,i_k})$, $\Lambda_{k,i_k} = \varepsilon_{k,i_k}(\hat{\bar{x}}_{k,i_k}) + d_{k,i_k}(t)$ and $|\Lambda_{k,i_k}| \le \overline{\Lambda}_{k,i_k}$ with $\overline{\Lambda}_{k,i_k}$ being the positive constant.

For the constrained fractional-order MIMO system (16), all the system states except $x_{k,1}$ are immeasurable, and a state observer must be designed to estimate the states. Then, the NN observer is constructed as

$$\begin{cases} \mathcal{D}^{\alpha} \hat{x}_{k,i_k} = h_{k,i_k} \hat{x}_{k,i_k+1} + \hat{\theta}_{k,i_k}^T S_{k,i_k}(\hat{\bar{x}}_{k,i_k}) + K_{k,i_k}(y_k - \hat{y}_k) \\ \mathcal{D}^{\alpha} \hat{x}_{k,n_k} = h_{k,n_k} u_k + \hat{\theta}_{k,n_k}^T S_{k,n_k}(\hat{\bar{x}}_{k,n_k}) + K_{k,n_k}(y_k - \hat{y}_k) \end{cases} \tag{17}$$

where K_{k,i_k} is the design parameter.

The estimation errors are defined as $\tilde{\theta}_{k,i_k} = \theta_{k,i_k} - \hat{\theta}_{k,i_k}$ and $\tilde{x}_{k,i_k} = x_{k,i_k} - \hat{x}_{k,i_k}$. By utilizing (16) and (17), one obtains

$$\mathcal{D}^{\alpha} \tilde{\bar{x}}_k = A_k \tilde{\bar{x}}_k + \sum_{i_k=1}^{n_k} \mathcal{B}_{i_k} \hat{\theta}_{k,i_k}^T S_{k,i_k}(\hat{\bar{x}}_{k,i_k}) + \Delta f_k(\hat{\bar{x}}_{k,i_k}) + \Lambda_k \tag{18}$$

where $\bar{x}_k = \begin{pmatrix} x_{1,i_k} & x_{2,i_k} & \cdots & x_{k,n_k} \end{pmatrix}^T$, $\Delta f_k = \left(\Delta f_{k,1}, \Delta f_{k,3}, \ldots, \Delta f_{k,n_k}\right)^T$, $\Lambda_k = \left(\Lambda_1, \Lambda_2, \ldots, \Lambda_{n_k}\right)^T$, $\mathcal{B}_{i_k} = \left(\underbrace{0 \cdots 1}_{i_k} \cdots 0\right)^T$ and $A_k = \begin{pmatrix} -K_{k,1} & h_{k,1} & \cdots & 0 \\ \vdots & \vdots & \ddots & \vdots \\ -K_{k,n_k-1} & 0 & \cdots & h_{k,n_k-1} \\ -K_{k,n_k} & 0 & \cdots & 0 \end{pmatrix}$, $K_k = \left[K_{k,1}, K_{k,2}, \ldots, K_{k,n_k}\right]^T$ should be properly chosen so that A_k is Hurwitz. There exists a matrix $P_k = P_k^T > 0$ satisfying:

$$A_k^T P_k + P_k A_k = -2Q_k \tag{19}$$

where $Q_k = Q_k^T > 0$.

Consider the Lyapunov candidate as $V_{k,e} = \tilde{x}_k^T P_k \tilde{x}_k$, and the $\alpha - order$ derivative of $V_{k,e}$ is presented as

$$\mathcal{D}^{\alpha} V_{k,e} = \tilde{x}_k^T \left(A_k^T P_k + P_k A_k\right) \tilde{x}_k + 2\tilde{x}_k P_k \left(\sum_{i_k=1}^{n_k} \mathcal{B}_{i_k} \hat{\theta}_{k,i_k}^T S_{k,i_k}(\hat{\bar{x}}_{k,i_k}) + \Delta f_k(\hat{\bar{x}}_{k,i_k}) + \Lambda_k \right) \tag{20}$$

According to Assumption 2 and Young's inequality, one can obtain

$$\begin{aligned} 2\tilde{x}_k P_k \Lambda_k &\le \tilde{x}_k^T \tilde{x}_k + \|P_k\|^2 \sum_{i_k=1}^{n_k} \overline{\Lambda}_{i_k}^2 \\ 2\tilde{x}_k P_k \Delta f_k &\le \left(1 + n_k c_k^2 \|P_k\|^2\right) \tilde{x}_k^T \tilde{x}_k \end{aligned} \tag{21}$$

where $c_k = \max\left\{c_{k,1}, c_{k,2}, \ldots, c_{k,n_k}\right\}$.

Based on the fact that $0 < S_{k,i_k}(\cdot)^T S_{k,i_k}(\cdot) < 1$, it follows that:

$$2\tilde{x}_k P_k \sum_{i_k=1}^{n_k} \mathcal{B}_{i_k} \hat{\theta}_{k,i_k}^T S_{k,i_k}(\hat{\bar{x}}_{k,i_k}) \le \lambda_{\max^2}(P_k) \tilde{x}_k^T \tilde{x}_k + \sum_{i_k=1}^{n_k} \tilde{\theta}_{i_k}^T \tilde{\theta}_{i_k} \tag{22}$$

Furthermore, substituting (21) and (22) into (20), we obtain

$$\mathcal{D}^{\alpha} V_{k,e} \le -\bar{q} \tilde{x}_k^T \tilde{x}_k + \sum_{i_k=1}^{n_k} \tilde{\theta}_{i_k}^T \tilde{\theta}_{i_k} + \|P_k\|^2 \sum_{i_k=1}^{n_k} \overline{\Lambda}_{i_k}^2 \tag{23}$$

where $\bar{q} = \lambda_{\min}(Q_k) - 2 - n_k c_k^2 \|P_k\|^2 - \lambda_{\max^2}(P_k)$.

5. Adaptive Controller Design

In this section, the prescribed performance adaptive tracking control approach will be designed, in which the barrier Lyapunov functions with the settling time regulator are employed to deal with the asymmetric full-state constraints.

Construct the asymmetric BLF as:

$$V_{k,z} = \frac{z_{k,1}^2}{\mathcal{F}_{k,2} - z_{k,1}} + \frac{z_{k,1}^2}{\mathcal{F}_{k,1} + z_{k,1}} \tag{24}$$

where $\mathcal{F}_{k,1}, \mathcal{F}_{k,2} > 0$. One can find that the boundedness of $V_{k,z}$ can ensure $-\mathcal{F}_{k,1} < z_{k,1} < \mathcal{F}_{k,2}$. Derive $\mathcal{D}^\alpha V_{k,z}$ as:

$$\mathcal{D}^\alpha V_{k,z} \le H_k z_{k,1}(\mathcal{D}^\alpha z_{k,1} + M_k) \tag{25}$$

where

$$\begin{aligned} H_k &= \tfrac{2\mathcal{F}_{k,2} - z_{k,1}}{(\mathcal{F}_{k,2} - z_{k,1})^2} + \tfrac{2\mathcal{F}_{k,1} + z_{k,1}}{(\mathcal{F}_{k,1} + z_{k,1})^2} \\ M_k &= \tfrac{z_{k,1}(\mathcal{F}_{k,2} - z_{k,1})^2}{G_k} \mathcal{D}^\alpha \mathcal{F}_{k,2} + \tfrac{z_{k,1}(\mathcal{F}_{k,1} + z_{k,1})^2}{G_k} \mathcal{D}^\alpha \mathcal{F}_{k,1} \\ G_k &= (2\mathcal{F}_{k,2} - z_{k,1})(\mathcal{F}_{k,1} + z_{k,1})^2 + (2\mathcal{F}_{k,1} + z_{k,1})(\mathcal{F}_{k,2} - z_{k,1})^2 \end{aligned}$$

Define the coordinate transformation as:

$$z_{k,1} = x_{k,1} - y_{k,d}, z_{k,i_k} = \hat{x}_{k,i_k} - \tau_{k,i_k,f}, e_{k,i_k} = \tau_{k,i_k,f} - \tau_{k,i_k-1} \tag{26}$$

where τ_{k,i_k-1} is the virtual controller, and $\tau_{k,i_k,f}$ is the filter signal from the filter.

According to (10), (18), and (26), the derivative of z_{k,i_k} is

$$\begin{aligned} \mathcal{D}^\alpha z_{k,1} &= h_{k,1} x_{k,2} + \theta_{k,1}^T S_{k,1}(\hat{\bar{x}}_{k,1}) + \Delta f_{k,1} + \Lambda_{k,1} - \mathcal{D}^\alpha y_{kd} \\ \mathcal{D}^\alpha z_{k,i_k} &= h_{k,i_k} \hat{x}_{k,i_k+1} + K_{k,i_k} \tilde{x}_{k,1} + \hat{\theta}_{k,i_k}^T S_{k,i_k}(\hat{\bar{x}}_{k,i_k}) - \mathcal{D}^\alpha \tau_{k,i_k,f} \\ \mathcal{D}^\alpha z_{k,n_k} &= h_{k,n_k} u_k + K_{k,n_k} \tilde{x}_{k,1} + \hat{\theta}_{k,n_k}^T S_{k,n_k}(\hat{\bar{x}}_{k,n_k}) - \mathcal{D}^\alpha \tau_{k,n_k,f} \end{aligned} \tag{27}$$

Step $(k,1)$: Define Lyapunov function candidate as

$$V_{k,1} = V_{k,e} + \frac{z_{k,1}^2}{\mathcal{F}_{k,1,2} - z_{k,1}} + \frac{z_{k,1}^2}{\mathcal{F}_{k,1,1} + z_{k,1}} + \frac{1}{2r_{k,1}} \tilde{\theta}_{k,1}^T \tilde{\theta}_{k,1} + \frac{e_{k,2}^2}{2} \tag{28}$$

where $r_{k,1} > 0$, $\mathcal{F}_{k,1,2} = \kappa_{k,1,2}\mathcal{P}_k(t)$, $\mathcal{F}_{k,1,1} = \kappa_{k,1,1}\mathcal{P}_k(t)$.

Based on (25), (27) and (28), one can obtain

$$\begin{aligned} \mathcal{D}^\alpha V_{k,1} &= \mathcal{D}^\alpha V_{k,e} + H_{k,1} z_{k,1}(\mathcal{D}^\alpha z_{k,1} + M_{k,1}) - r_{k,1}^{-1} \tilde{\theta}_{k,1}^T \mathcal{D}^\alpha \hat{\theta}_{k,1} + e_{k,2} \mathcal{D}^\alpha e_{k,2} \\ &\le -\bar{q} \tilde{x}_k^T \tilde{x}_k + \sum_{i_k=1}^{n_k} \tilde{\theta}_{i_k}^T \tilde{\theta}_{i_k} + \|P_k\|^2 \sum_{i_k=1}^{n_k} \overline{\Lambda}_{i_k}^2 + H_{k,1} z_{k,1} \Big(h_{k,1} x_{k,2} + \theta_{k,1}^T S_{k,1}(\hat{\bar{x}}_{k,1}) \\ &+ \Delta f_{k,1} + \Lambda_{k,1} - \mathcal{D}^\alpha y_{kd} + M_{k,1} \Big) - r_{k,1}^{-1} \tilde{\theta}_{k,1}^T \mathcal{D}^\alpha \hat{\theta}_{k,1} + e_{k,2} \mathcal{D}^\alpha e_{k,2} \end{aligned} \tag{29}$$

where

$$\begin{aligned} M_{k,1} &= \tfrac{z_{k,1} \mathcal{D}^\alpha \mathcal{F}_{k,1,2}}{G_{k,1}} + \tfrac{z_{k,1} \mathcal{D}^\alpha \mathcal{F}_{k,1,1}}{G_{k,1}} \\ H_{k,1} &= \tfrac{2\mathcal{F}_{k,1,2} - z_{k,1}}{(\mathcal{F}_{k,1,2} - z_{k,1})^2} + \tfrac{2\mathcal{F}_{k,1,1} + z_{k,1}}{(\mathcal{F}_{k,1,1} + z_{k,1})^2} \\ G_{k,1} &= (2\mathcal{F}_{k,1,2} - z_{k,1})(\mathcal{F}_{k,1,1} + z_{k,1})^2 + (2\mathcal{F}_{k,1,1} + z_{k,1})(\mathcal{F}_{k,1,2} - z_{k,1})^2 \end{aligned}$$

Due to Young's inequality, one can have

$$\begin{aligned} h_{k,1}H_{k,1}z_{k,1}(z_{k,2}+e_{k,2}+\widetilde{x}_{k,2}) &\le \tfrac{5}{4}h_{k,1}^2H_{k,1}^2z_{k,1}^2+\tfrac{e_{k,2}^2}{2}+\tfrac{1}{2}\widetilde{x}_k^T\widetilde{x}_k+z_{k,2}^2 \\ H_{k,1}z_{k,1}(\Delta f_{k,1}+\Lambda_{k,1}) &\le H_{k,1}^2z_{k,1}^2+\tfrac{c_{k,1}^2}{2}\widetilde{x}_k^T\widetilde{x}_k+\tfrac{\overline{\Lambda}_{k,1}^2}{2} \end{aligned} \tag{30}$$

The virtual controller $\tau_{k,1}$ and law $\hat{\theta}_{k,1}$ are designed as

$$\begin{aligned} \tau_{k,1} &= -h_{k,1}^{-1}\left(b_{k,1}z_{k,1}+\left(1+\tfrac{5h_{k,1}^2}{4}\right)H_{k,1}z_{k,1}+\hat{\theta}_{k,1}S_{k,1}(\hat{\widetilde{x}}_{k,1})-\mathcal{D}^\alpha y_{k,d}+M_{k,1}\right) \\ \mathcal{D}^\alpha\hat{\theta}_{k,1} &= r_{k,1}H_{k,1}z_{k,1}S_{k,1}(\hat{\widetilde{x}}_{k,1})-\sigma_{k,1}\hat{\theta}_{k,1} \end{aligned} \tag{31}$$

where $b_{k,1},\sigma_{k,1}>0$. Based on (29)–(31) and the fact that $\frac{\sigma_{k,1}}{r_{k,1}}\widetilde{\theta}_{k,1}^T\hat{\theta}_{k,1}=-\frac{\sigma_{k,1}}{2r_{k,1}}\widetilde{\theta}_{k,1}^T\widetilde{\theta}_{k,1}+\frac{\sigma_{k,1}}{2r_{k,1}}\theta_{k,1}^T\theta_{k,1}$ yields

$$\begin{aligned} \mathcal{D}^\alpha V_{k,1} \le{}& -\overline{q}_{k,1}\widetilde{x}_k^T\widetilde{x}_k+\sum_{i_k=1}^{n_k}\widetilde{\theta}_{i_k}^T\widetilde{\theta}_{i_k}{}_i-\frac{\sigma_{k,1}}{2r_{k,1}}\widetilde{\theta}_{k,1}^T\widetilde{\theta}_{k,1}-b_{k,1}H_{k,1}z_{k,1}^2+z_{k,2}^2 \\ &+\frac{e_{k,2}^2}{2}+e_{k,2}\mathcal{D}^\alpha e_{k,2}+\|P_k\|^2\sum_{i_k=1}^{n_k}\overline{\Lambda}_{i_k}^2+\frac{\sigma_{k,1}}{2r_{k,1}}\widetilde{\theta}_{k,1}^T\widetilde{\theta}_{k,1}+\frac{\overline{\Lambda}_{k,1}^2}{2} \end{aligned} \tag{32}$$

where $\overline{q}_{k,1}=\overline{q}-\frac{1+c_{k,1}^2}{2}$.

The fractional-order filter can be designed as:

$$\varsigma_{k,2}D^\alpha\tau_{k,2,f}+\tau_{k,2,f}=\tau_{k,1},\tau_{k,2,f}(0)=\tau_{k,1}(0) \tag{33}$$

where $\varsigma_{k,2}>0$.

According to (26) and (33), one can obtain

$$\mathcal{D}^\alpha e_{k,2}=\mathcal{D}^\alpha\tau_{k,2,f}-\mathcal{D}^\alpha\tau_{k,1}=-\frac{e_{k,2}}{\varsigma_{k,2}}-\mathcal{D}^\alpha\tau_{k,1} \tag{34}$$

It is assumed that $\left|\mathcal{D}^\alpha\tau_{k,1}\right|\le-\Psi_{k,1}(Y_{k,1})$, where $\Psi_{k,1}(Y_{k,1})$ is a continuous function and $Y_{k,1}=\left(z_{k,1},\hat{\theta}_{k,1},\mathcal{D}^\alpha\hat{\theta}_{k,1},y_{k,d},\mathcal{D}^\alpha y_{k,d},\mathcal{D}^\alpha(\mathcal{D}^\alpha y_{k,d}),\mathcal{F}_{k,1,1},\mathcal{D}^\alpha\mathcal{F}_{k,1,1},\mathcal{D}^\alpha(\mathcal{D}^\alpha\mathcal{F}_{k,1,1}),\mathcal{D}^\alpha\mathcal{F}_{k,1,2},\mathcal{F}_{k,1,2},\mathcal{D}^\alpha(\mathcal{D}^\alpha\mathcal{F}_{k,1,2})\right)^T$.

Subsequently, adopting Young's inequality, we obtain

$$e_{k,2}D^\alpha e_{k,2}\le-\frac{e_{k,2}^2}{\varsigma_{k,2}}+\frac{e_{k,2}^2}{2}+\frac{\Psi_{k,1}^2}{2} \tag{35}$$

Thus, the inequality (32) is restated as

$$\mathcal{D}^\alpha V_{k,1}\le-\overline{q}_{k,1}\widetilde{x}_k^T\widetilde{x}_k+\sum_{i_k=1}^{n_k}\widetilde{\theta}_{i_k}^T\widetilde{\theta}_{i_k}{}_i-\frac{\sigma_{k,1}}{2r_{k,1}}\widetilde{\theta}_{k,1}^T\widetilde{\theta}_{k,1}-b_{k,1}H_{k,1}z_{k,1}^2+z_{k,2}^2-a_{k,2}e_{k,2}^2+\frac{\Psi_{k,1}^2}{2}+\Xi_{k,1} \tag{36}$$

where $\Xi_{k,1}=\|P_k\|^2\sum_{i_k=1}^{n_k}\overline{\Lambda}_{i_k}^2+\frac{\sigma_{k,1}}{2r_{k,1}}\widetilde{\theta}_{k,1}^T\widetilde{\theta}_{k,1}+\frac{\overline{\Lambda}_{k,1}^2}{2}$ and $a_{k,2}$ is a positive constant guaranteeing $\frac{1}{\varsigma_{k,2}}>1+a_{k,2}$.

Step $(k,i_k),2\le i_k\le n_k-1$: Consider the Lyapunov function presented below

$$V_{k,i_k}=V_{k,i_k-1}+\frac{z_{k,i_k}^2}{\mathcal{F}_{k,i_k,2}-z_{k,i_k}}+\frac{z_{k,i_k}^2}{\mathcal{F}_{k,i_k,1}+z_{k,i_k}}+\frac{1}{2r_{k,i_k}}\widetilde{\theta}_{k,i_k}^T\widetilde{\theta}_{k,i_k}+\frac{e_{k,i_k+1}^2}{2} \tag{37}$$

where $r_{k,i_k}>0$ are some constants, and $\mathcal{F}_{k,i_k,1}$ and $\mathcal{F}_{k,i_k,2}$ are to be created later on. The $\alpha-order$ derivative of V_{k,i_k} is organized as

$$\begin{aligned}\mathcal{D}^{\alpha}V_{k,i_k} &= \mathcal{D}^{\alpha}V_{k,i_k-1} + H_{k,i_k}\mathrm{z}_{k,i_k}\mathcal{D}^{\alpha}\mathrm{z}_{k,i_k} - r_{k,i_k}^{-1}\widetilde{\theta}_{k,i_k}^{T}\mathcal{D}^{\alpha}\hat{\theta}_{k,i_k} + e_{k,i_k+1}\mathcal{D}^{\alpha}e_{k,i_k+1}\\ &\le -\overline{q}_{k,i_k-1}\widetilde{x}_k^{T}\widetilde{x}_k + \sum_{j=1}^{n_k}\widetilde{\theta}_{k,j}^{T}\widetilde{\theta}_{k,j} - \sum_{j=1}^{i_k-1}\frac{\sigma_{k,j}}{2r_{k,j}}\widetilde{\theta}_{k,j}^{T}\widetilde{\theta}_{k,j} - \sum_{j=1}^{i_k-1}b_{k,j}H_{k,j}\mathrm{z}_{k,j}^{2}\\ &\quad - \sum_{j=2}^{i_k-1}a_{k,j}e_{k,j}^{2} + \sum_{j=2}^{i_k}\frac{\Psi_{k,j}^{2}}{2} + \Xi_{k,i_k-1} + \mathrm{z}_{k,i_k}^{2} + \sum_{j=2}^{i_k-1}\frac{1}{2}\widetilde{\theta}_{k,j}^{T}\widetilde{\theta}_{k,j} - r_{k,i_k}^{-1}\widetilde{\theta}_{k,i_k}^{T}\mathcal{D}^{\alpha}\hat{\theta}_{k,i_k}\\ &\quad + H_{k,i_k}\mathrm{z}_{k,i_k}\left(h_{k,i_k}\hat{x}_{k,i_k+1} + K_{k,i_k}\widetilde{x}_{k,1} + \hat{\theta}_{k,i_k}^{T}S_{k,i_k}\left(\hat{\widetilde{x}}_{k,i_k}\right) - \mathcal{D}^{\alpha}\tau_{k,i_k,f}\right) + e_{k,i_k+1}\mathcal{D}^{\alpha}e_{k,i_k+1}\end{aligned} \tag{38}$$

where

$$H_{k,i_k} = \frac{2\mathcal{F}_{k,i_k,2} - \mathrm{z}_{k,i_k}}{\left(\mathcal{F}_{k,i_k,2} - \mathrm{z}_{k,i_k}\right)^{2}} + \frac{2\mathcal{F}_{k,i_k,1} - \mathrm{z}_{k,i_k}}{\left(\mathcal{F}_{k,i_k,1} - \mathrm{z}_{k,i_k}\right)^{2}}$$

Construct the virtual controller and adaptive law as

$$\begin{aligned}\tau_{k,i_k-1} &= -h_{k,i_k}^{-1}\left(\left(1 + b_{k,i_k} + \left(\frac{3h_{k,i_k}^{2}}{4} + \frac{K_{k,i_k}^{2}}{4} + \frac{1}{2}\right)H_{k,i_k}\right)\mathrm{z}_{k,i_k} + \hat{\theta}_{k,i_k}^{T}S_{k,i_k}\left(\hat{\widetilde{x}}_{k,i_k}\right) - \mathcal{D}^{\alpha}\tau_{k,i_k,f}\right)\\ \mathcal{D}^{\alpha}\hat{\theta}_{k,i_k} &= r_{k,i_k}H_{k,i_k}\mathrm{z}_{k,i_k}S_{k,i_k}\left(\hat{\widetilde{x}}_{k,i_k}\right) - \sigma_{k,i_k}\hat{\theta}_{k,i_k}\end{aligned} \tag{39}$$

where $b_{k,i_k}, \sigma_{k,i_k} > 0$.

Then, one can have

$$\begin{aligned}h_{k,i_k}H_{k,i_k}\mathrm{z}_{k,i_k}\left(\mathrm{z}_{k,i_k+1} + e_{k,i_k+1}\right) &\le \tfrac{3}{4}h_{k,i_k}^{2}H_{k,i_k}^{2}\mathrm{z}_{k,i_k}^{2} + \tfrac{e_{k,i_k+1}^{2}}{2} + \mathrm{z}_{k,i_k+1}^{2}\\ H_{k,i_k}\mathrm{z}_{k,i_k}\left(K_{k,i_k}\widetilde{x}_{k,1} - \widetilde{\theta}_{k,i_k}^{T}S_{k,i_k}\left(\hat{\widetilde{x}}_{k,i_k}\right)\right) &\le \left(\tfrac{K_{k,i_k}^{2}}{4} + \tfrac{1}{2}\right)H_{k,i_k}^{2}\mathrm{z}_{k,i_k}^{2} + \widetilde{x}_k^{T}\widetilde{x}_k + \tfrac{1}{2}\widetilde{\theta}_{k,i_k}^{T}\widetilde{\theta}_{k,i_k}\end{aligned} \tag{40}$$

Due to $\frac{\sigma_{k,i_k}}{r_{k,i_k}}\widetilde{\theta}_{k,i_k}^{T}\hat{\theta}_{k,i_k} = -\frac{\sigma_{k,i_k}}{2r_{k,i_k}}\widetilde{\theta}_{k,i_k}^{T}\widetilde{\theta}_{k,i_k} + \frac{\sigma_{k,i_k}}{2r_{k,i_k}}\theta_{k,i_k}^{T}\theta_{k,i_k}$ and (38), one can obtain

$$\begin{aligned}\mathcal{D}^{\alpha}V_{k,i_k} &\le -\overline{q}_{k,i_k}\widetilde{x}_k^{T}\widetilde{x}_k + \sum_{j=1}^{n_k}\widetilde{\theta}_{k,j}^{T}\widetilde{\theta}_{k,j} - \sum_{j=1}^{i_k-1}\frac{\sigma_{k,j}}{2r_{k,j}}\widetilde{\theta}_{k,j}^{T}\widetilde{\theta}_{k,j} + \sum_{j=2}^{i_k-1}\frac{1}{2}\widetilde{\theta}_{k,j}^{T}\widetilde{\theta}_{k,j}\\ &\quad - \sum_{j=1}^{i_k-1}b_{k,j}H_{k,j}\mathrm{z}_{k,j}^{2} - \sum_{j=2}^{i_k-1}a_{k,j}e_{k,j}^{2} + \sum_{j=2}^{i_k}\frac{\Psi_{k,j}^{2}}{2} + \Xi_{k,i_k} + \mathrm{z}_{k,i_k}^{2} + e_{k,i_k+1}\mathcal{D}^{\alpha}e_{k,i_k+1}\end{aligned} \tag{41}$$

where $\overline{q}_{k,i_k} = \overline{q}_{k,i_k-1} - 1$ and $\Xi_{k,i_k} = \Xi_{k,i_k-1} + \frac{\sigma_{k,i_k}}{2r_{k,i_k}}\theta_{k,i_k}^{T}\theta_{k,i_k}$.

Design the fractional-order filter as

$$\varsigma_{k,i_k+1}D^{\alpha}\tau_{k,i_k,f} + \tau_{k,i_k,f} = \tau_{k,i_k-1}, \tau_{k,i_k,f}(0) = \tau_{k,i_k}(0) \tag{42}$$

Then, one can have

$$\mathcal{D}^{\alpha}e_{k,i_k+1} = \mathcal{D}^{\alpha}\tau_{k,i_k,f} - \mathcal{D}^{\alpha}\tau_{k,i_k-1} = -\frac{e_{k,i_k+1}}{\varsigma_{k,i_k+1}} - D^{\alpha}\tau_{k,i_k-1} \tag{43}$$

Assume $\left|D^{\alpha}\tau_{k,i_k-1}\right| \le -\Psi_{k,i_k}\left(Y_{k,i_k}\right)$, where $\Psi_{k,i_k}\left(Y_{k,i_k}\right)$ is a continuous function and $Y_{k,i_k} = \left(\mathrm{z}_{k,i_k}, \hat{\theta}_{k,i_k}, \mathcal{D}^{\alpha}\hat{\theta}_{k,i_k}\right)^{T}$. Then

$$e_{k,i_k+1}\mathcal{D}^{\alpha}e_{k,i_k+1} \le -\frac{e_{k,i_k+1}^{2}}{\varsigma_{k,i_k+1}} + \frac{e_{k,i_k+1}^{2}}{2} + \frac{1}{2}\Psi_{k,i_k} \tag{44}$$

Based on (41) and (44), one can obtain

$$\begin{aligned}\mathcal{D}^{\alpha}V_{k,i_k} &\le -\overline{q}_{k,i_k}\widetilde{x}_k^{T}\widetilde{x}_k + \sum_{j=1}^{n_k}\widetilde{\theta}_{k,j}^{T}\widetilde{\theta}_{k,j} - \sum_{j=1}^{i_k-1}\frac{\sigma_{k,j}}{2r_{k,j}}\widetilde{\theta}_{k,j}^{T}\widetilde{\theta}_{k,j} + \sum_{j=2}^{i_k-1}\frac{1}{2}\widetilde{\theta}_{k,j}^{T}\widetilde{\theta}_{k,j}\\ &\quad - \sum_{j=1}^{i_k-1}b_{k,j}H_{k,j}\mathrm{z}_{k,j}^{2} - \sum_{j=2}^{i_k-1}a_{k,j}e_{k,j}^{2} + \sum_{j=2}^{i_k}\frac{\Psi_{k,j}^{2}}{2} + \Xi_{k,i_k} + \mathrm{z}_{k,i_k}^{2}\end{aligned} \tag{45}$$

where $a_{k,i_k+1} > 0$, satisfying $\frac{1}{\varsigma_{k,i_k+1}} > 1 + a_{k,i_k+1}$.

Step (k, n_k): Select the Lyapunov function as:

$$V_{k,n_k} = V_{k,n_k-1} + \frac{z_{k,n_k}^2}{\mathcal{F}_{k,n_k,2} - z_{k,n_k}} + \frac{z_{k,n_k}^2}{\mathcal{F}_{k,n_k,1} + z_{k,n_k}} + \frac{1}{2r_{k,n_k}}\widetilde{\theta}_{k,n_k}^T\widetilde{\theta}_{k,n_k} \tag{46}$$

where $r_{k,n_k} > 0$, and $\mathcal{F}_{k,n_k,1}$ and $\mathcal{F}_{k,n_k,2}$ will be given later.

From (46), one can have

$$\begin{aligned}\mathcal{D}^\alpha V_{k,n_k} &= \mathcal{D}^\alpha V_{k,n_k-1} + H_{k,n_k} z_{k,n_k}\mathcal{D}^\alpha z_{k,n_k} - r_{k,n_k}^{-1}\widetilde{\theta}_{k,n_k}^T\mathcal{D}^\alpha\hat{\theta}_{k,n_k}\\ &\le -\overline{q}_{k,n_k-1}\widetilde{x}_k^T\widetilde{x}_k + \sum_{j=1}^{n_k}\widetilde{\theta}_{k,j}^T\widetilde{\theta}_{k,j}\widetilde{\theta}_{k,j} - \sum_{j=1}^{n_k-1}\frac{\sigma_{k,j}}{2r_{k,j}}\widetilde{\theta}_{k,j}^T\widetilde{\theta}_{k,j} - \sum_{j=1}^{n_k-1} b_{k,j}H_{k,j}z_{k,j}^2\\ &\quad - \sum_{j=2}^{n_k} a_{k,j}e_{k,j}^2 + \sum_{j=2}^{n_k}\frac{\Psi_{k,j}^2}{2} + \sum_{j=2}^{n_k-1}\frac{1}{2}\widetilde{\theta}_{k,j}^T\widetilde{\theta}_{k,j} + \Xi_{k,n_k-1} + z_{k,n_k}^2 - r_{k,n_k}^{-1}\widetilde{\theta}_{k,n_k}^T\mathcal{D}^\alpha\hat{\theta}_{k,n_k}\\ &\quad + H_{k,n_k}z_{k,n_k}\left(h_{k,n_k}u_k + K_{k,n_k}\widetilde{x}_{k,1} + \hat{\theta}_{k,n_k}^T S_{k,n_k}(\hat{\widetilde{x}}_{k,n_k}) - \mathcal{D}^\alpha\tau_{k,n_k,f}\right)\end{aligned} \tag{47}$$

where $H_{k,n_k} = \left(2\mathcal{F}_{k,n_k,2} - z_{k,n_k}\right)/\left(\mathcal{F}_{k,n_k,2} - z_{k,n_k}\right)^2 + \left(2\mathcal{F}_{k,n_k,1} + z_{k,n_k}\right)/\left(\mathcal{F}_{k,n_k,1} + z_{k,n_k}\right)^2$.

Design the actual control signal u_k and the adaptation law $\hat{\theta}_{k,n_k}$ as

$$\begin{aligned}u_k &= -h_{k,n_k}^{-1}\left((1+b_{k,n_k})z_{k,n_k} + \left(\frac{K_{k,n_k}^2}{4} + \frac{1}{2}\right)H_{k,n_k}z_{k,n_k} + \hat{\theta}_{k,n_k}^T S_{k,n_k}(\hat{\widetilde{x}}_{k,n_k}) - \mathcal{D}^\alpha\tau_{k,n_k,f}\right)\\ \mathcal{D}^\alpha\hat{\theta}_{k,n_k} &= r_{k,n_k}H_{k,n_k}z_{k,n_k}S_{k,n_k}(\hat{\widetilde{x}}_{k,n_k}) - \sigma_{k,n_k}\hat{\theta}_{k,n_k}\end{aligned} \tag{48}$$

where $b_{k,n_k}, \sigma_{k,n_k} > 0$.

Using Young's inequality, one has

$$H_{k,n_k}z_{k,n_k}\left(K_{k,n_k}\widetilde{x}_1 - \widetilde{\theta}_{k,n_k}^T S_{k,n_k}(\hat{\widetilde{x}}_{k,n_k})\right) \le \left(\frac{K_{k,n_k}^2}{4} + \frac{1}{2}\right)H_{k,n_k}^2 z_{k,n_k}^2 + \widetilde{x}_k^T\widetilde{x}_k + \frac{1}{2}\widetilde{\theta}_{k,n_k}^T\widetilde{\theta}_{k,n_k} \tag{49}$$

Consequently, due to $\frac{\sigma_{k,n_k}}{r_{k,n_k}}\widetilde{\theta}_{k,n_k}^T\hat{\theta}_{k,n_k} = -\frac{\sigma_{k,n_k}}{2r_{k,n_k}}\widetilde{\theta}_{k,n_k}^T\widetilde{\theta}_{k,n_k} + \frac{\sigma_{k,n_k}}{2r_{k,n_k}}\theta_{k,n_k}^T\theta_{k,n_k}$, it can be further deduced that

$$\begin{aligned}\mathcal{D}^\alpha V_{k,n_k} &\le -\overline{q}_{k,n_k}\widetilde{x}_k^T\widetilde{x}_k + \sum_{i_k=1}^{n_k}\widetilde{\theta}_{k,i_k}^T\widetilde{\theta}_{k,i_k} - \sum_{i_k=1}^{n_k}\frac{\sigma_{k,i_k}}{2r_{k,i_k}}\widetilde{\theta}_{k,i_k}^T\widetilde{\theta}_{k,i_k}\\ &\quad + \sum_{i_k=2}^{n_k}\frac{1}{2}\widetilde{\theta}_{k,i_k}^T\widetilde{\theta}_{k,i_k} - \sum_{i_k=1}^{n_k} b_{k,i_k}H_{k,i_k}z_{k,i_k}^2 - \sum_{i_k=2}^{n_k} a_{k,i_k}e_{k,i_k}^2 + \sum_{i_k=2}^{n_k}\frac{\Psi_{k,i_k}^2}{2} + \Xi_{k,n_k}\end{aligned} \tag{50}$$

where $\overline{q}_{k,n_k} = \overline{q}_{k,n_k-1} - 1$ and $\Xi_{k,n_k} = \Xi_{k,n_k-1} + \frac{\sigma_{k,n_k}}{2}\theta_{k,n_k}^T\theta_{k,n_k}$.

Theorem 1. *Consider the fractional-order MIMO nonlinear system (10) under Assumptions 1 and 2, if an adaptive controller and adaptive laws (31), (39) and (48) with state observer (17) are designed, for any* $x_{k,i_k}(0) \in \mathfrak{D}_{x_{k,i_k}}$*, one can obtain that all the signals closed-loop system are bounded; the practical prescribed time tracking and the states confined to predetermined constraints are guaranteed.*

Proof. For $z_{k,i_k} \in \Omega_{z_{k,i_k}}$, one can obtain

$$\begin{aligned}H_{k,i_k}z_{k,i_k}^2 &= \frac{2\mathcal{F}_{k,i_k,2} - z_{k,i_k}}{\left(\mathcal{F}_{k,i_k,2} - z_{k,i_k}\right)^2}z_{k,i_k}^2 + \frac{2\mathcal{F}_{k,i_k,1} + z_{k,i_k}}{\left(\mathcal{F}_{k,i_k,1} + z_{k,i_k}\right)^2}z_{k,i_k}^2\\ &\ge \frac{z_{k,i_k}^2}{\mathcal{F}_{k,i_k,2} - z_{k,i_k}} + \frac{z_{k,i_k}^2}{\mathcal{F}_{k,i_k,1} + z_{k,i_k}} + N\end{aligned} \tag{51}$$

where $N = \frac{\mathcal{F}_{k,i_k,2}\mathrm{z}_{k,i_k}^2}{\left(\mathcal{F}_{k,i_k,2}-\mathrm{z}_{k,i_k}\right)^2} + \frac{\mathcal{F}_{k,i_k,1}\mathrm{z}_{k,i_k}^2}{\left(\mathcal{F}_{k,i_k,1}+\mathrm{z}_{k,i_k}\right)^2} \geq 0$. Thus, one can obtain

$$-b_{k,i_k}H_{k,i_k}\mathrm{z}_{k,i_k}^2 \leq -\frac{b_{k,i_k}\mathrm{z}_{k,i_k}^2}{\mathcal{F}_{k,i_k,2}-\mathrm{z}_{k,i_k}} - \frac{b_{k,i_k}\mathrm{z}_{k,i_k}^2}{\mathcal{F}_{k,i_k,1}+\mathrm{z}_{k,i_k}} \tag{52}$$

Define the compact sets as: $\Omega_{y_{k,d}} = \left\{(y_{k,d}, \mathcal{D}^\alpha y_{k,d}, \mathcal{D}^\alpha(\mathcal{D}^\alpha y_{k,d}))^T : y_{k,d}^2 + (\mathcal{D}^\alpha y_{k,d})^2 + (\mathcal{D}^\alpha(\mathcal{D}^\alpha y_{k,d}))^2 \leq \omega_{y_{k,d}}\right\}$ and $\Omega_{V_{k,i_k}} = \left\{\widetilde{x}_k^T P_k \widetilde{x}_k + \sum_{i_k=1}^{n_k} \widetilde{\theta}_{k,i_k}^T \widetilde{\theta}_{k,i_k} + \sum_{i_k=2}^{n_k} e_{k,i_k}^2 + \sum_{i_k=1}^{n_k}\left(\frac{\mathrm{z}_{k,i_k}^2}{\mathcal{F}_{k,i_k,2}-\mathrm{z}_{k,i_k}} + \frac{\mathrm{z}_{k,i_k}^2}{\mathcal{F}_{k,i_k,1}+\mathrm{z}_{k,i_k}}\right) \leq \mathrm{C}_{k,i_k}\right\}$ with $\omega_{y_{k,d}}, C_{k,i_k} > 0$. Then, $\Psi_{k,i_k}(Y_{k,i_k}) \leq D_{k,i_k}$ with $D_{k,i_k} > 0$ on compact set $\Omega_{V_{k,i_k}} \times \Omega_{y_{k,d}}$.

Consider Lyapunov function as: $V = \sum_{k=1}^{l} V_{k,n_k}$. From (50), one can obtain

$$\begin{aligned}
\mathcal{D}^\alpha V &= \sum_{k=1}^{l} \mathcal{D}^\alpha V_{k,n_k} \\
&\leq -\sum_{k=1}^{l} \overline{q}_{k,n_k}\widetilde{x}_k^T\widetilde{x}_k + \sum_{k=1}^{l}\sum_{i_k=1}^{n_k} \widetilde{\theta}_{k,i_k}^T\widetilde{\theta}_{k,i_k} - \sum_{k=1}^{l}\sum_{i_k=1}^{n_k} \frac{\sigma_{k,i_k}}{2r_{k,i_k}}\widetilde{\theta}_{k,i_k}^T\widetilde{\theta}_{k,i_k} + \sum_{k=1}^{l}\sum_{i_k=2}^{n_k} \frac{1}{2}\widetilde{\theta}_{k,i_k}^T\widetilde{\theta}_{k,i_k} \\
&\quad - \sum_{k=1}^{l}\sum_{i_k=2}^{n_k} a_{k,i_k}e_{k,i_k}^2 + \sum_{k=1}^{l}\sum_{i_k=2}^{n_k} \frac{D_{k,i_k}^2}{2} - \sum_{k=1}^{l}\sum_{i_k=1}^{n_k} b_{k,i_k}\left(\frac{\mathrm{z}_{k,i_k}^2}{\mathcal{F}_{k,i_k,2}-\mathrm{z}_{k,i_k}} + \frac{\mathrm{z}_{k,i_k}^2}{\mathcal{F}_{k,i_k,1}+\mathrm{z}_{k,i_k}}\right) + \sum_{k=1}^{l}\Xi_{k,n_k} \\
&\leq -\beta V + \gamma
\end{aligned} \tag{53}$$

where

$$\begin{aligned}
&\gamma = \sum_{k=1}^{l}\sum_{i_k=2}^{n_k} \frac{D_{k,i_k}^2}{2} + \sum_{k=1}^{l}\Xi_{k,n_k} \\
&\beta = \min\left\{\frac{\overline{q}_{k,n_k}}{\lambda_{\max}(P_k)}, b_{k,i_k}, 2\left(\frac{\sigma_{k,1}}{2r_{k,1}}-1\right), 2\left(\frac{\sigma_{k,j_k+1}}{2r_{k,j_k+1}}-\frac{3}{2}\right), 2a_{k,j_k+1}\right\} \\
&k = 1,2,\ldots,l; i_k = 1,2,\ldots,n_k; j_k = 1,2,\ldots,n_k-1.
\end{aligned} \tag{54}$$

(1) Define $\mathfrak{B}(t)$ satisfying

$$\mathcal{D}^\alpha V + \mathfrak{B}(t) = -\beta V + \gamma \tag{55}$$

From Definition 2, the Laplace transform of (55) is

$$V(s) = \frac{s^{\alpha-1}}{s^\alpha+\beta}V(0) - \frac{1}{s^\alpha+\beta}\mathfrak{B}(s) + \frac{\gamma}{s(s^\alpha+\beta)} \tag{56}$$

where $V(s) = L\{V(t)\}$ and $\mathfrak{B}(s) = L\{\mathfrak{B}(t)\}$. By using Laplace's inverse transformation, one can have

$$V(t) = V(0)E_{\alpha,1}(-\beta t^\alpha) + \gamma t^\alpha E_{\alpha,\alpha+1}(-\beta t^\alpha) - \mathfrak{B}(t) * t^{\alpha-1}E_{\alpha,\alpha}(-\beta t^\alpha) \tag{57}$$

From Lemma 4, one can obtain $-\mathfrak{B}(t) * t^{\alpha-1}E_{\alpha,\alpha}(-\beta t^\alpha) \leq 0$, $\gamma t^\alpha E_{\alpha,\alpha+1}(-\beta t^\alpha) \leq \gamma/\beta$, and

$$V(t) \leq V(0)E_{\alpha,1}(-\beta t^\alpha) + \frac{\gamma}{\beta} \leq \mathcal{H} \tag{58}$$

where $\mathcal{H} = V(0) + \frac{\gamma}{\beta} > 0$.

Therefore, V is bounded, and $\widetilde{x}_{k,i_k}, \mathrm{z}_{k,i_k}, \widetilde{\theta}_{k,i_k}$ and e_{k,i_k} are also bounded.

(2) Due to $\mathrm{z}_{k,1}$ being bounded, one can have $-\kappa_{k,1,1}\mathcal{P}_k(t) \leq \mathrm{z}_{k,1}(t) \leq -\kappa_{k,2,1}\mathcal{P}_k(t)$. According to $\mathcal{P}_k(t)$ in (9), it is true that $\left|\mathrm{z}_{k,1}\right| \leq \epsilon_k$ for $t > T_k$. Then, the tracking errors keep the predefined performance with parameters ϵ_k and T_k.

(3) Due to $\mathrm{z}_{k,j_k}, \hat{\theta}_{k,j_k}$ and $e_{k,j_k}(j_k = 1,2,\ldots,n_k)$ being bounded, $\tau_{k,i_k,f}(i_k = 2,3,\ldots,n_k)$ in (31) and (39) is also bounded and satisfies $\aleph_{k,i_k,1} < \tau_{k,i_k,f} < \aleph_{k,i_k,2}$, where $\aleph_{k,i_k,1}$ and $\aleph_{k,i_k,2}$ are some constants. Due to boundedness of $\widetilde{x}_{k,i_k}$, assume $\hbar_{k,i_k,1} < \widetilde{x}_{k,i_k} <$

$\hbar_{k,i_k,2}$, where $\hbar_{k,i_k,1}$ and $\hbar_{k,i_k,2}$ are some constants. Using $z_{k,i_k} = \hat{x}_{k,i_k} - \tau_{k,i_k,f}$, $\widetilde{x}_{k,i_k} = x_{k,i_k} - \hat{x}_{k,i_k}$ and $-\kappa_{k,i_k,1} < x_{k,i_k} < \kappa_{k,i_k,2}$, one can have $-\mathcal{F}_{k,i_k,1} + \aleph_{k,i_k,1} + \hbar_{k,i_k,1} < x_{k,i_k} < \mathcal{F}_{k,i_k,2} + \aleph_{k,i_k,2} + \hbar_{k,i_k,2}$. Define $\mathcal{F}_{k,i_k,1} = k_{k,i_k,1} + \aleph_{k,i_k,1} + \hbar_{k,i_k,1}$ and $\mathcal{F}_{k,i_k,2} = k_{k,i_k,2} - \aleph_{k,i_k,2} - \hbar_{k,i_k,2}$, one has $-\kappa_{k,i_k,1} < x_{k,i_k} < \kappa_{k,i_k,2}$. The proof ends here. □

Remark 3. *From (58), we can obtain* $\left|z_{k,i_k}\right| \leq \sqrt{\mathcal{F}V_n(0) + \mathcal{F}\gamma/\beta}$ *with* $\mathcal{F} = \max_{i_k=1,\ldots,n_k;k=1,\ldots l} \left\{\mathcal{F}_{k,i_k,1} + \mathcal{F}_{k,i_k,2}\right\}$, $\left|e_{k,j_k}\right| \leq \sqrt{2V_n(0) + 2\gamma/\beta}$, $\left\|\widetilde{\theta}_{k,i_k}\right\| \leq \sqrt{2r_{k,i_k}V_n(0) + 2r_{k,i_k}\gamma/\beta}$, $i_k = 1,\ldots,n_k; k = 1,\ldots l; j_k = 2,\ldots,n_k$, *and the upper bounds of* $z_{k,i_k}, \widetilde{\theta}_{k,i_k}$ *and* e_{k,j_k} *can be reduced by increasing* β *or decreasing* γ*, which can be achieved by selecting appropriate parameters* $\overline{q}_{k,n_k}, b_{k,i_k}, \sigma_{k,i_k}, r_{k,i_k}$ *and* a_{k,i_k} *due to the definitions of* γ *and* β *in (54). The performance function found in (9) shows* T_k, k_a *and* m*, in which the tracking performance improved by reducing* k_a *and* T_k *improves, but that may come at the cost of the bigger control signals. Furthermore, the* σ_{k,i_k} *reflects the convergence rate of* $\hat{\theta}_{k,i_k}$*, in which it may not be enough to prevent parameter estimation drift when* σ_{k,i_k} *is too small. Therefore, in practical applications, it is often necessary to strike a balance between proper control efforts and satisfactory tracking performance.*

To clarify the system's components and the interactions, the schematic diagram of the proposed method is shown in Figure 1.

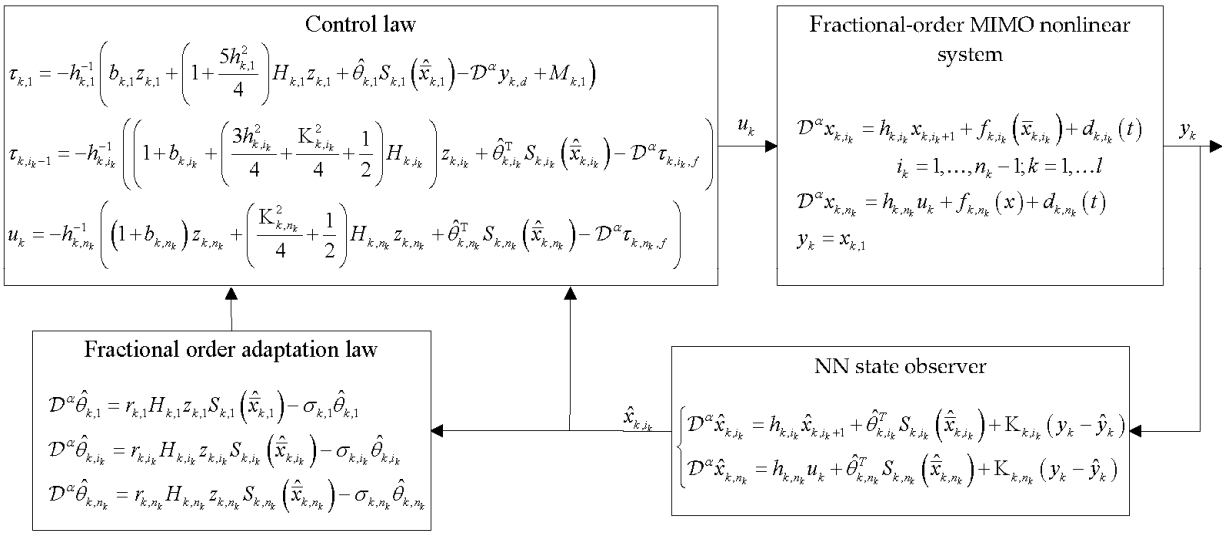

Figure 1. The schematic diagram of the proposed method.

6. Simulation Results

In this section, two fractional-order numerical simulation examples are performed to illustrate the reliability and validity of the proposed tracking control strategy.

6.1. Example 1

Consider a fractional-order nonlinear MIMO system modeled as:

$$\begin{cases} \mathcal{D}^\alpha x_{1,1} = 0.8x_{1,2} + \frac{x_{1,1}^3\cos(x_{1,1})}{1+x_{1,1}} - 0.01\sin(2t) \\ \mathcal{D}^\alpha x_{1,2} = 1.5u_1 - 0.02x_{1,2} - \sin(x_{1,1}x_{2,2}) + 0.3\sin(x_{1,1})\cos(x_{1,2}) + 0.02\cos(t) \end{cases} \tag{59}$$

and

$$\begin{cases} \mathcal{D}^\alpha x_{2,1} = 0.6x_{2,2} + \cos\left(x_{2,1}^4x_{2,2}\right) + 0.05\cos(0.1t) \\ \mathcal{D}^\alpha x_{2,2} = 2.6u_2 + 0.5\cos(x_{2,1}x_{2,2})\sin\left(0.5x_{1,2}x_{2,2}^3\right) - 0.01\sin(0.6t) \end{cases} \tag{60}$$

where $\alpha = 0.6$. Assumptions 1–2 are satisfied for the systems (59) and (60). The initial states are $x_{1,1}(0) = x_{1,2}(0) = x_{2,1}(0) = x_{2,2}(0) = 0$. The constrained sets are chosen as $\kappa_{1,1,1} = \kappa_{1,1,2} = 0.35$, $\kappa_{1,2,1} = 1.3$, $\kappa_{1,2,2} = 1.35$, $\kappa_{2,1,1} = 0.65$, $\kappa_{2,1,2} = 0.85$, $\kappa_{2,2,1} = 0.5$, $\kappa_{2,2,2} = 2.9$. The desired output trajectory signals are chosen as $y_{1,d} = 0.3\sin(10t)\cos(5t) + 0.01$ and $y_{2,d} = 0.5\sin(8t)\cos(3t) + 0.05$.

The design parameters are shown as: $K_{1,1} = 21, K_{1,2} = 11, K_{2,1} = 61, K_{2,2} = 11, b_{1,1} = 15$, $b_{1,2} = 5$, $b_{2,1} = 15$, $b_{2,2} = 5,5$, $r_{1,1} = r_{1,2} = r_{2,1} = r_{2,2} = 0.01$, $\sigma_{1,1} = \sigma_{1,2} = \sigma_{2,1} = \sigma_{2,2} = 0.001$, $T_1 = T_2 = 2$, $k_a = 0.45$, and $m = 3.2$.

Figures 2–6 show the simulation results. The trajectories of system outputs, reference signals, and the predefined constraints are presented in Figure 2 to show the tracking performance of the closed-loop fractional-order system. It demonstrates that the reference signals $y_{1,d}, y_{2,d}$ could be tracked well by the output signals $x_{1,1}, x_{2,1}$ staying within the predefined constraints, respectively. Figure 2 displays the trajectories of system states $x_{1,2}, x_{2,2}$ and state estimations $\hat{x}_{1,2}, \hat{x}_{2,2}$, respectively. It can be found that $\hat{x}_{1,2}, \hat{x}_{2,2}$ can estimate $x_{1,2}, x_{2,2}$, respectively, which all stay in the predefined constraints all the time. Figure 4 shows the response curves of the errors $z_{1,1}$ and $z_{2,1}$, which converge to the compact sets $\Omega_b = \{z_1 || z_{1,1}| < 0.015\}$ and $\Omega_c = \{z_{2,1} || z_1| < 0.02\}$ within 2s, respectively. Figure 5 shows the norm of parameters estimation of the RBF NN, and system control inputs u_1 and u_2 are presented in Figure 6, which are all bounded. It is clear that the state constraints and prescribed tracking performance are fulfilled, and all the signals in the closed-loop fractional-order system are bounded.

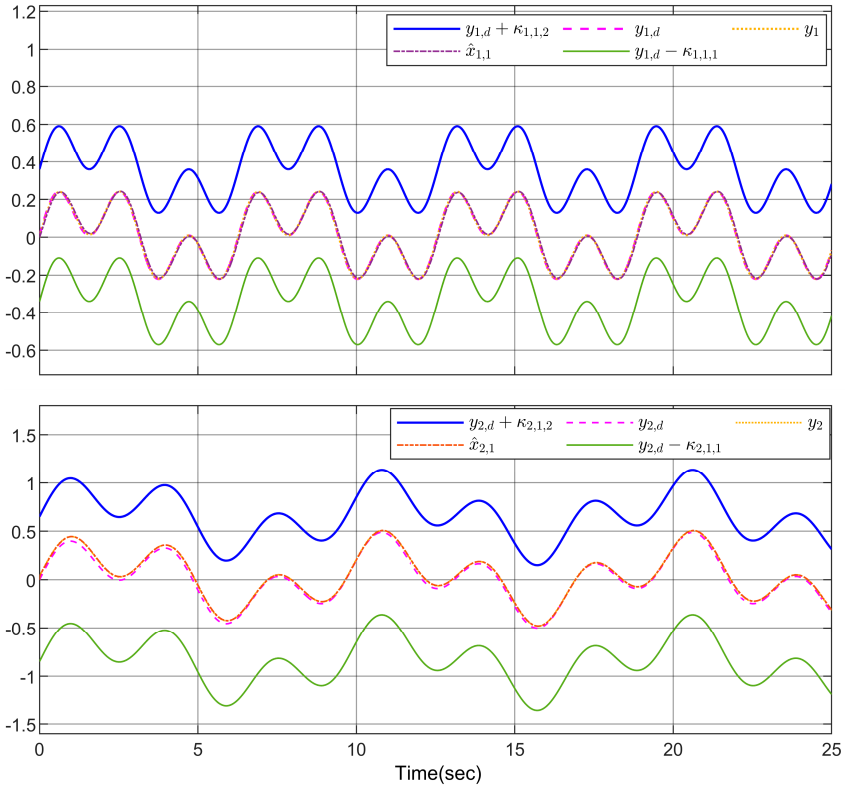

Figure 2. The trajectories of desired signals and system outputs.

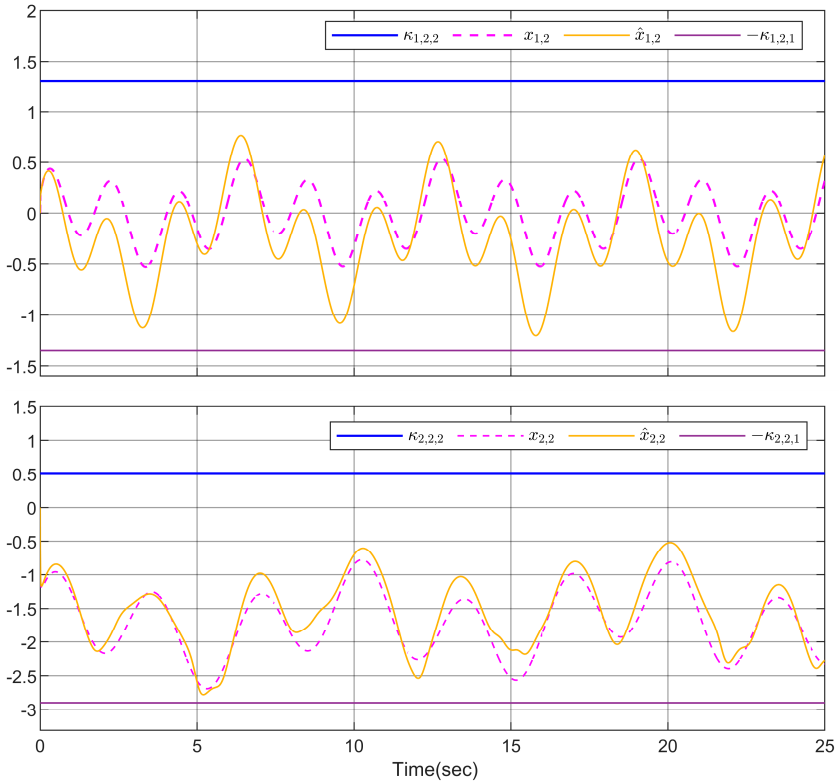

Figure 3. The trajectories of system states $x_{1,2}, x_{2,2}$ and state estimations $\hat{x}_{1,2}, \hat{x}_{2,2}$.

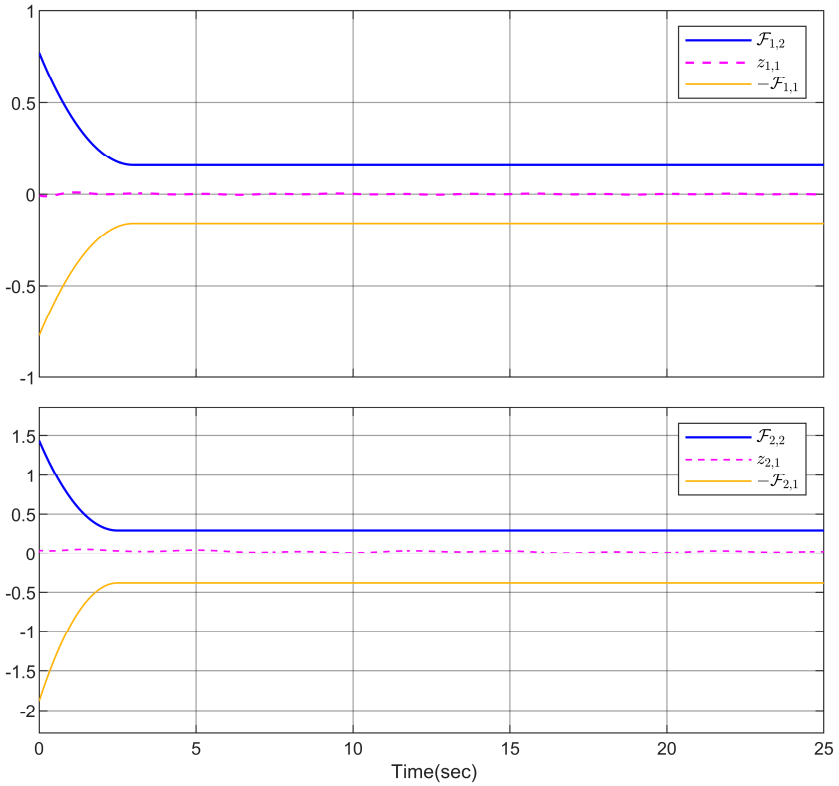

Figure 4. The trajectories of the errors $z_{1,1}$ and $z_{2,1}$.

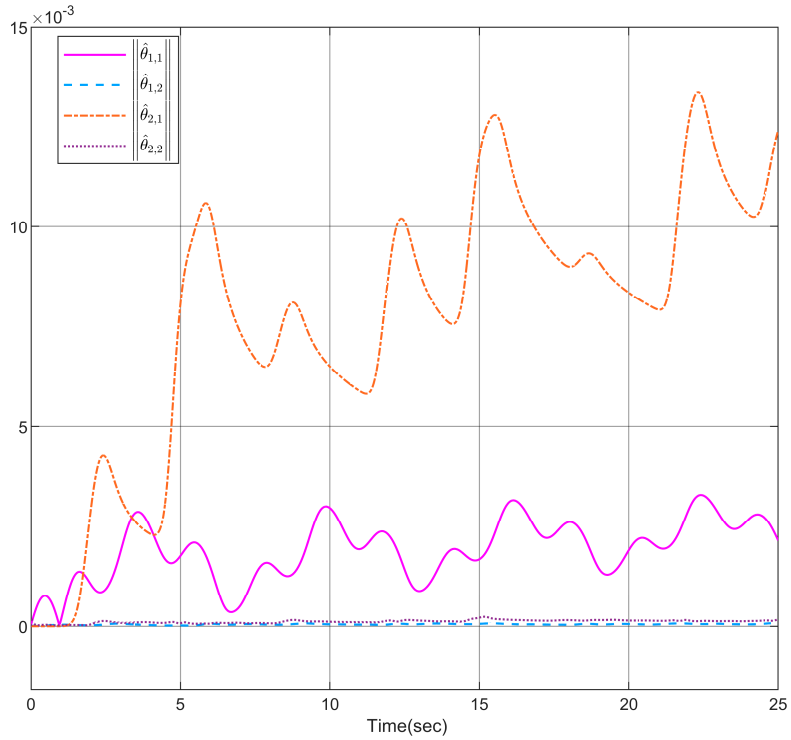

Figure 5. The norm of parameters estimation.

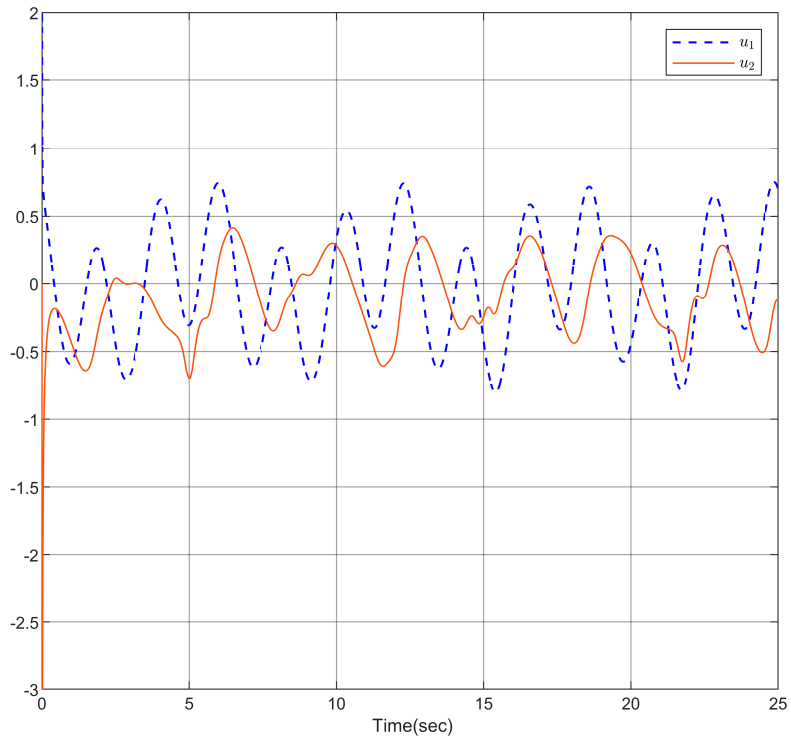

Figure 6. The trajectories the control inputs u_1 and u_2.

6.2. Example 2 (Permanent Magnet Synchronous Motor System)

Consider the fractional-order permanent magnet synchronous motor (PMSM) model as follows [52]:

$$\begin{cases} \mathcal{D}^{0.91}\varpi = k(i_q - \varpi) \\ \mathcal{D}^{0.91}i_q = -i_q - \varpi i_d + \vartheta\varpi + h_1 u_q \\ \mathcal{D}^{0.91}i_d = -i_d - \varpi i_q + h_2 u_d \end{cases} \tag{61}$$

where ϖ represents the angular velocity of the rotor. For $d-q$ axis currents, i_d and i_q are variables. u_d and u_q denote the voltages. $\vartheta = 1, k = 4, h_1 = 20$ and $h_2 = 15$ are parameters.

Define $x_{1,1} = \varpi, x_{1,2} = i_q, u_1 = u_q, x_{2,1} = i_d, u_2 = u_d$, then the PMSM system can be considered as the following two subsystems as:

$$\begin{cases} \mathcal{D}^{0.91} x_{1,1} = k(x_{1,2} - x_{1,1}) + d_{1,1}(t) \\ \mathcal{D}^{0.91} x_{1,2} = -x_{1,2} - x_{1,1}x_{1,2} + \vartheta x_{1,1} + h_1 u_1 + d_{1,2}(t) \\ y_1 = x_{1,1} \end{cases} \tag{62}$$

and

$$\begin{cases} \mathcal{D}^{0.91} x_{2,1} = -x_{2,1} - x_{1,1}x_{2,1} + h_2 u_2 + d_{2,1}(t) \\ y_2 = x_{2,1} \end{cases} \tag{63}$$

Choose the parameters as $\kappa_{1,1,1} = \kappa_{1,1,2} = 0.35$, $\kappa_{1,2,1} = \kappa_{1,2,2} = 1.5$, $\kappa_{2,1,1} = 1.65$, $\kappa_{2,1,2} = 1.85$. $K_{1,1} = 181$, $K_{1,2} = 11$, $K_{2,1} = 31$, $b_{1,1} = 15$, $b_{1,2} = 3$, $b_{2,1} = 15$, $r_{1,1} = r_{1,2} = r_{2,1} = 0.001$, $T_1 = T_2 = 0.5$, $\sigma_{1,1} = \sigma_{1,2} = \sigma_{2,1} = 0.002$, $k_a = 0.43$, and $m = 3.5$. The outputs track to the desired trajectory $y_{1,d} = 0.85\sin(0.6t)$ and $y_{2,d} = 0.85\cos(0.6t)$.

To illustrate the validity of the proposed method, an adaptive backstepping control scheme (ABCS) is used for comparison from [53]. The simulation results are shown in Figures 7–11. Figure 7 presents the trajectories of system outputs, reference signals, and the predefined constraints to show the tracking performance of the closed-loop fractional-order system. It demonstrates that the reference signals $y_{1,d}, y_{2,d}$ could be tracked well by the output signals $x_{1,1}, x_{2,1}$ staying within the predefined constraints, respectively. the trajectories of system states $x_{1,2}, x_{2,2}$ and state estimations $\hat{x}_{1,2}$ is displayed in Figure 8, respectively. It can be found that $\hat{x}_{1,2}$ can estimate $x_{1,2}$, which are all stay in the predefined constraints all the time. The response curves of the errors $z_{1,1}$ and $z_{2,1}$ are shown in Figure 9, which converge to the compact sets $\Omega_b = \{z_1 | |z_{1,1}| < 0.2\}$ and $\Omega_c = \{z_{2,1} | |z_1| < 1\}$ within 0.5s, respectively. The norm of parameter estimation of the RBF NN is shown in Figure 10, and system control inputs u_1 and u_2 are presented in Figure 11, which are all bounded.

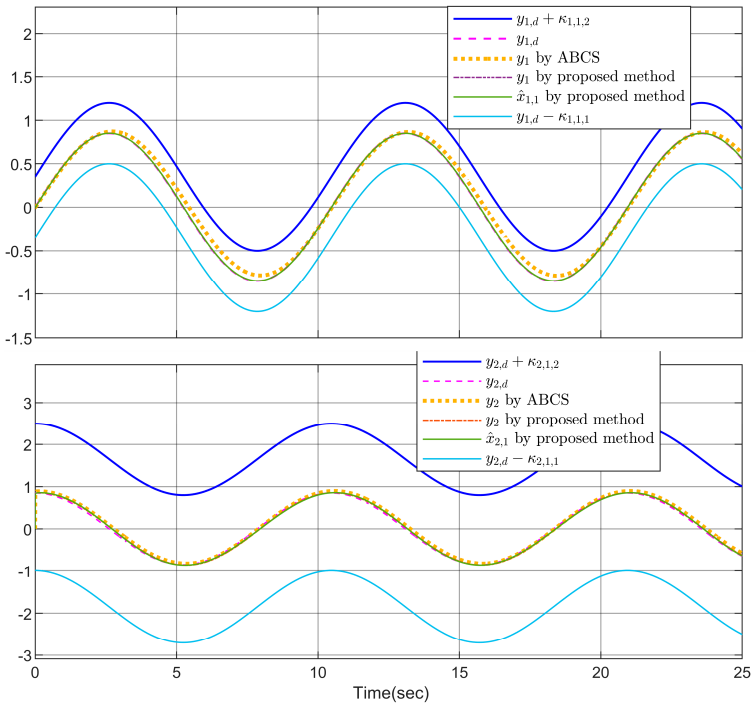

Figure 7. The trajectories of desired signals and system outputs.

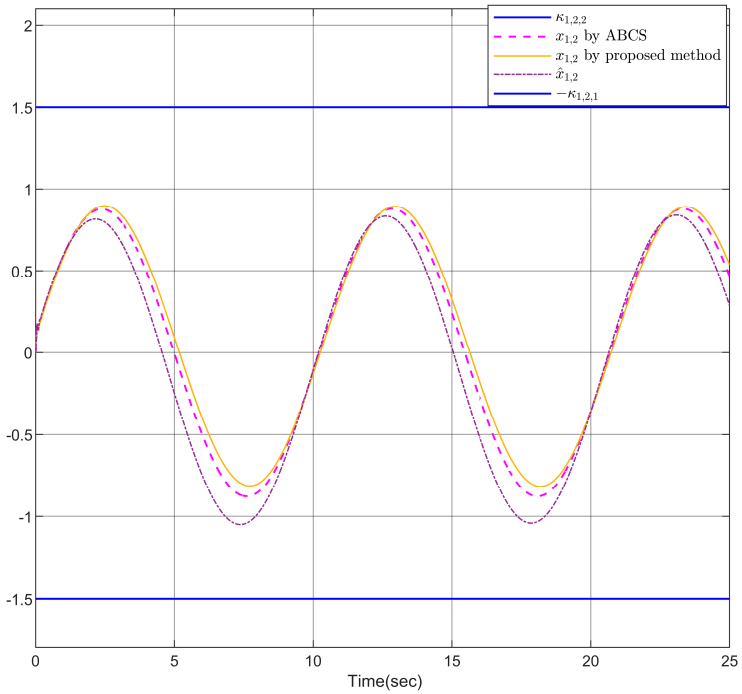

Figure 8. The trajectories of system state $x_{1,2}$ and state estimation $\hat{x}_{1,2}$.

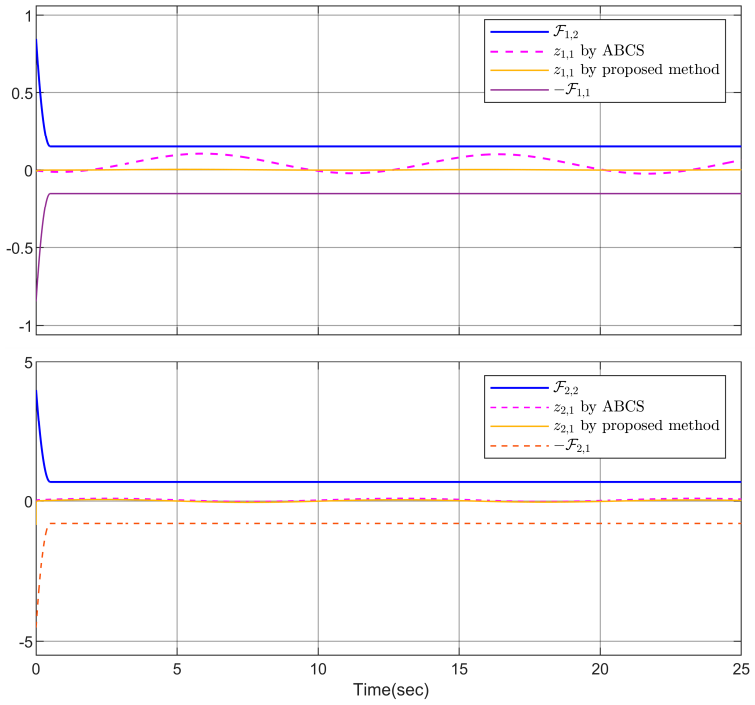

Figure 9. The trajectories of the errors $z_{1,1}$ and $z_{2,1}$.

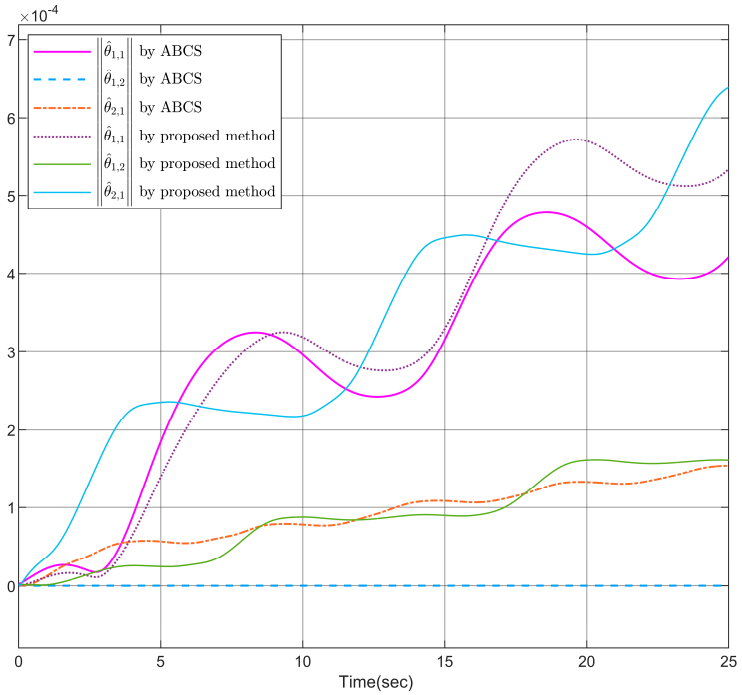

Figure 10. The norm of parameters estimation.

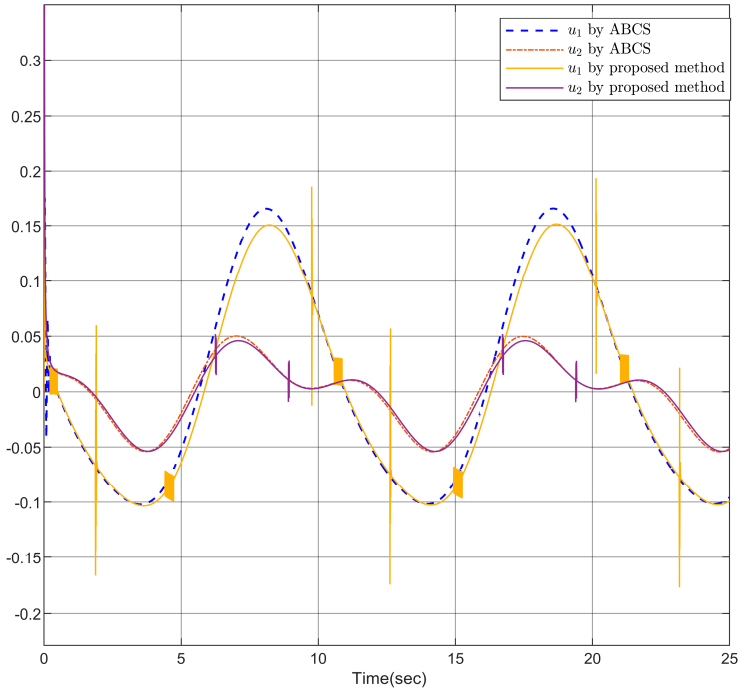

Figure 11. The trajectories the control inputs u_1 and u_2.

The overall tracking error $OTE = \sqrt{\sum_{k=1}^{2} z_{k,1}^2(X)}$ is defined to compare the performance under different external disturbances, where X is the sample index. Table 1 shows the OTE by the proposed method and ABCS. Obviously, the proposed method can have better tracking accuracy compared with ABCS.

Table 1. Performance comparisons.

Disturbances	OTE by ABCS	OTE by Proposed Method
$d_{1,1}(t) = d_{1,2}(t) = d_{2,1}(t) = 0$	0.0526	0.0026
$d_{1,1}(t) = 0.01\sin(t)$ $d_{1,2}(t) = 0.01\cos(t)$ $d_{2,1}(t) = 0.01\sin(1.5t)$	0.1835	0.0139
$d_{1,1}(t) = 0.1\sin(t)$ $d_{1,2}(t) = 0.1\cos(t)$ $d_{2,1}(t) = 0.1\sin(1.5t)$	0.3261	0.0675

Based on the above simulation results, it is clear that the state constraints and prescribed tracking performance are fulfilled, and all the signals in the closed-loop fractional-order system are bounded by using the proposed method.

7. Conclusions

A prescribed performance tracking control scheme is developed for the fractional-order nonlinear MIMO under systems with asymmetric full-state constraints and unmeasurable system states. The NN nonlinear state observer is developed to estimate the unmeasurable states. The asymmetric BLFs with the settling time regulator are presented to deal with asymmetric full-state constraints and achieve the tracking accuracy in the predefined time. The stability analysis for closed-loop fractional-order MIMO system is presented on the basis of the fractional-order stability theory. The simulation examples including fractional-order PMSM system illustrate the validity of the proposed scheme. In the future, the scalability or performance in the fractional-order large-scale systems will be considered and investigated, and the practical applications will be implemented as far as possible.

Author Contributions: Conceptualization, S.L. and T.Y.; methodology, S.L.; software, S.L.; validation, T.Y.; formal analysis, T.Y.; investigation, S.L.; writing—original draft preparation, T.Y.; writing—review and editing, S.L.; visualization, S.L.; supervision, C.W.; funding acquisition, T.Y. All authors have read and agreed to the published version of the manuscript.

Funding: This work was supported by Shandong Provincial Natural Science Foundation of China (ZR2024ME219).

Data Availability Statement: Data are contained within the article.

Conflicts of Interest: The authors declare no conflicts of interest.

References

1. Zhou, Q.; Ren, Q.; Ma, H.; Chen, G.; Li, H. Model-Free Adaptive Control for Nonlinear Systems Under Dynamic Sparse Attacks and Measurement Disturbances. *IEEE Trans. Circuits Syst. I Regul. Pap.* **2024**, *71*, 4731–4741. [CrossRef]
2. Meng, T.; Zhang, Y.; Fu, Q.; Wang, J. Observer-Based Adaptive Control for a Coupled PDE–ODE System of a Flexible Wing. *IEEE Trans. Syst. Man Cybern. Syst.* **2024**, *54*, 3949–3959. [CrossRef]
3. Cheng, Y.; Zhang, Y.; Chu, H.; Yu, Q.; Gao, B.; Chen, H. Safety-Critical Control of 4WDEV Trajectory Tracking via Adaptive Control Barrier Function. *IEEE Trans. Transp. Electrif.* **2024**, 1–11. [CrossRef]
4. Wang, Y.; Duan, G.; Li, P. Event-Triggered Adaptive Control of Uncertain Strict-Feedback Nonlinear Systems Using Fully Actuated System Approach. *IEEE Trans. Cybern.* **2024**, 1–13. [CrossRef]
5. Lu, K.; Liu, Z.; Yu, H.; Chen, C.L.P.; Zhang, Y. A small-gain approach to inverse optimal adaptive control of nonlinear systems with unmodeled dynamics. *Automatica* **2024**, *159*, 111360. [CrossRef]
6. Tran, V.P.; Mabrok, M.A.; Anavatti, S.G.; Garratt, M.A.; Petersen, I.R. Robust Adaptive Fuzzy Control for Second-Order Euler–Lagrange Systems with Uncertainties and Disturbances via Nonlinear Negative-Imaginary Systems Theory. *IEEE Trans. Cybern.* **2024**, *54*, 5102–5114. [CrossRef]
7. Liu, M.; Zhang, W. Disturbance observer-based adaptive fuzzy control for pure-feedback systems with deferred output constraints. *Nonlinear Dyn.* **2024**, 1–18. [CrossRef]
8. Zhao, Z.; Feng, K.; Wang, X.; Yang, C.; Li, X.; Hong, K.S. Adaptive NN Control for a Flexible Manipulator with Input Backlash and Output Constraint. *IEEE Trans. Syst. Man Cybern. Syst.* **2024**, 1–10. [CrossRef]

9. Zong, G.; Wang, Y.; Niu, B.; Su, S.F.; Shi, K. Event-triggered adaptive NN tracking control for nonlinear systems with asymmetric time-varying output constraints and application to an AUVs. *IEEE Trans. Veh. Technol.* **2024**, 1–11. [CrossRef]
10. Yang, X.; Yan, J.; Chen, C.; Hua, C.; Guan, X. Adaptive Asymptotic Tracking Control for Underactuated Autonomous Underwater Vehicles with State Constraints. *IEEE Trans. Intell. Transp. Syst.* **2024**, 1–16. [CrossRef]
11. Chen, J.; Mu, D.; Hua, C.; Luo, X.; Zhang, Y.; Sun, F. Adaptive Tracking Control for Uncertain Unmanned Fire Fighting Robot with Input Saturation and Full-State Constraints. *IEEE Trans. Intell. Transp. Syst.* **2024**, *25*, 12776–12783. [CrossRef]
12. Liu, Y.; Chen, Z.; Yao, B. Online Optimization-Based Time-Optimal Adaptive Robust Control of Linear Motors with Input and State Constraints. *IEEE/ASME Trans. Mechatron.* **2024**, *29*, 3157–3165. [CrossRef]
13. Guo, H.; Peng, W.; Zhang, M.; Li, C.; Li, Z. Adaptive control for 5-DOF varying-cable-length tower cranes with multivariable state constraints. *Nonlinear Dyn.* **2024**, 1–19. [CrossRef]
14. Chao, D.; Qi, R.; Jiang, B. Adaptive Integrated Guidance and Control for HSV in Ascent Phase with Time-Varying State Constraints. *IEEE Trans. Aerosp. Electron. Syst.* **2024**, 1–18. [CrossRef]
15. Chen, G.; Dong, J. Approximate Optimal Adaptive Prescribed Performance Control for Uncertain Nonlinear Systems with Feature Information. *IEEE Trans. Syst. Man Cybern. Syst.* **2024**, *54*, 2298–2308. [CrossRef]
16. Guo, G.; Zhang, C.L. Adaptive Fault-Tolerant Control with Global Prescribed Performance of Strict-Feedback Systems. *IEEE Trans. Syst. Man Cybern. Syst.* **2024**, *54*, 4832–4840. [CrossRef]
17. Song, X.; Sun, P.; Song, S.; Stojanovic, V. Saturated-threshold event-triggered adaptive global prescribed performance control for nonlinear Markov jumping systems and application to a chemical reactor model. *Expert. Syst. Appl.* **2024**, *249*, 123490. [CrossRef]
18. Liu, Z.; Zhao, Y.; Zhang, O.; Gao, Y.; Liu, J. Adaptive fuzzy neural network-based finite time prescribed performance control for uncertain robotic systems with actuator saturation. *Nonlinear Dyn.* **2024**, *112*, 12171–12190. [CrossRef]
19. Hu, C.; Wang, Z.; Bu, X.; Zhao, J.; Na, J.; Gao, H. Optimal Tracking Control for Autonomous Vehicle with Prescribed Performance via Adaptive Dynamic Programming. *IEEE Trans. Intell. Transp. Syst.* **2024**, *25*, 12437–12449. [CrossRef]
20. Li, P.; Gao, R.; Xu, C.; Li, Y.; Akgül, A.; Baleanu, D. Dynamics exploration for a fractional-order delayed zooplankton–phytoplankton system. *Chaos Solitons Fractals* **2023**, *166*, 112975. [CrossRef]
21. Yavuz, M.; Özköse, F.; Susam, M.; Kalidass, M. A New Modeling of Fractional-Order and Sensitivity Analysis for Hepatitis-B Disease with Real Data. *Fractal Fract.* **2023**, *7*, 165. [CrossRef]
22. Farman, M.; Sarwar, R.; Akgul, A. Modeling and analysis of sustainable approach for dynamics of infections in plant virus with fractal fractional operator. *Chaos Solitons Fractals* **2023**, *170*, 113373. [CrossRef]
23. Qu, J.; Zhang, Q.; Yang, A.; Chen, Y.; Zhang, Q. Variational fractional-order modeling of viscoelastic axially moving plates and vibration simulation. *Commun. Nonlinear Sci. Numer. Simul.* **2024**, *130*, 107707. [CrossRef]
24. Song, P.; Wei, P.; Zhou, X. Vibration of rectangular plate on fractional order viscoelastic foundation subjected to standing and moving loads. *Mech. Time-Depend. Mater.* **2024**, *28*, 541–561. [CrossRef]
25. Teimouri, H.; Faal, R.T.; Milani, A.S. Impact response of fractionally damped rectangular plates made of viscoelastic composite materials. *Appl. Math. Model.* **2025**, *137*, 115678. [CrossRef]
26. Lin, Z.; He, L.; Zhou, H. Adaptive Low-Order Harmonic Currents Suppression in AC Power System Using Fractional-Order Circuit. *IEEE Trans. Circuits Syst. I Regul. Pap.* **2024**, *71*, 4446–4457. [CrossRef]
27. Shukla, H.; Raju, M. Combined frequency and voltage regulation in an interconnected power system using fractional order cascade controller considering renewable energy sources, electric vehicles and ultra capacitor. *J. Energy Storage* **2024**, *84*, 110875. [CrossRef]
28. Guha, D.; Roy, P.K.; Banerjee, S. Adaptive fractional-order sliding-mode disturbance observer-based robust theoretical frequency controller applied to hybrid wind–diesel power system. *ISA Trans.* **2023**, *133*, 160–183. [CrossRef]
29. Li, Q.; Li, R.; Huang, D. Dynamic analysis of a new 4D fractional-order financial system and its finite-time fractional integral sliding mode control based on RBF neural network. *Chaos Solitons Fractals* **2023**, *177*, 114156. [CrossRef]
30. Gao, W.; Veeresha, P.; Baskonus, H.M. Dynamical analysis fractional-order financial system using efficient numerical methods. *Appl. Math. Sci. Eng.* **2023**, *31*, 2155152. [CrossRef]
31. Zhang, X.; Zhang, W.; Cao, J.; Liu, H. Observer-based command filtered adaptive fuzzy control for fractional-order MIMO nonlinear systems with unknown dead zones. *Expert. Syst. Appl.* **2024**, *255*, 124623. [CrossRef]
32. Aguila-Camacho, N.; Gallegos, J.A. Error-Based Switched Fractional Order Model Reference Adaptive Control for MIMO Linear Time Invariant Systems. *Fractal Fract.* **2024**, *8*, 109. [CrossRef]
33. Wang, L.; Liu, D.-Y.; Gibaru, O. A new modulating functions-based non-asymptotic state estimation method for fractional-order systems with MIMO. *Nonlinear Dyn.* **2023**, *111*, 5533–5546. [CrossRef]
34. Bai, Z.; Li, S.; Liu, H. Observer-based fuzzy event-triggered control for state constrained MIMO fractional-order systems. *Expert. Syst. Appl.* **2024**, *256*, 124915. [CrossRef]
35. Zhao, D.; Hu, Y.; Sun, W.; Zhou, X.; Xu, L.; Yan, S. A digraph approach to the state-space model realization of MIMO non-commensurate fractional order systems. *J. Frankl. Inst.* **2022**, *359*, 5014–5035. [CrossRef]
36. Lin, F.; Xue, G.; Qin, B.; Li, S.; Liu, H. Event-triggered finite-time fuzzy control approach for fractional-order nonlinear chaotic systems with input delay. *Chaos Solitons Fractals* **2023**, *175*, 114036. [CrossRef]
37. Qu, Y.; Ji, Y. Fractional-order finite-time sliding mode control for uncertain teleoperated cyber–physical system with actuator fault. *ISA Trans.* **2024**, *144*, 61–71. [CrossRef]

38. Zhou, B.; Zhang, Z.; Michiels, W. Functional and dual observer based prescribed-time control of linear systems by periodic delayed feedback. *Automatica* **2024**, *159*, 111406. [CrossRef]
39. Obuz, S.; Selim, E.; Tatlicioglu, E.; Zergeroglu, E. Robust Prescribed Time Control of Euler–Lagrange Systems. *IEEE Trans. Ind. Electron.* **2024**, 1–8. [CrossRef]
40. Singh, V.K.; Kamal, S.; Bandyopadhyay, B.; Ghosh, S.; Dinh, T.N. Prescribed-Time Optimal Control of Nonlinear Dynamical Systems with Application to a Coupled Tank System. *IEEE Trans. Autom. Sci. Eng.* **2024**, 1–11. [CrossRef]
41. Cheng, H.; Huang, X.; Li, Z. Unified neuroadaptive fault-tolerant control of fractional-order systems with or without state constraints. *Neurocomputing* **2023**, *524*, 117–125. [CrossRef]
42. Song, S.; Park, J.H.; Zhang, B.; Song, X. Observer-Based Adaptive Hybrid Fuzzy Resilient Control for Fractional-Order Nonlinear Systems with Time-Varying Delays and Actuator Failures. *IEEE Trans. Fuzzy Syst.* **2021**, *29*, 471–485. [CrossRef]
43. Podlubny, I. *Fractional Differential Equations*; Academic: New York, NY, USA, 1999.
44. Zouari, F.; Ibeas, A.; Boulkroune, A.; Cao, J.; Arefi, M.M. Neuro-adaptive tracking control of non-integer order systems with input nonlinearities and time-varying output constraints. *Inf. Sci.* **2019**, *485*, 170–199. [CrossRef]
45. Wei, M.; Li, Y.-X.; Tong, S. Event-triggered adaptive neural control of fractional-order nonlinear systems with full-state constraints. *Neurocomputing* **2020**, *412*, 320–326. [CrossRef]
46. Cao, Y.; Cao, J.; Song, Y. Practical Prescribed Time Control of Euler–Lagrange Systems with Partial/Full State Constraints: A Settling Time Regulator-Based Approach. *IEEE Trans. Cybern.* **2022**, *52*, 13096–13105. [CrossRef]
47. Bingi, K.; Rajanarayan Prusty, B.; Pal Singh, A. A Review on Fractional-Order Modelling and Control of Robotic Manipulators. *Fractal Fract.* **2023**, *7*, 77. [CrossRef]
48. Homaeinezhad, M.R.; Shahhosseini, A. Fractional order actuation systems: Theoretical foundation and application in feedback control of mechanical systems. *Appl. Math. Model.* **2020**, *87*, 625–639. [CrossRef]
49. Yu, Z.; Sun, Y.; Dai, X. Stability and Stabilization of the Fractional-Order Power System with Time Delay. *IEEE Trans. Circuits Syst. II Express Briefs* **2021**, *68*, 3446–3450. [CrossRef]
50. Alilou, M.; Azami, H.; Oshnoei, A.; Mohammadi-Ivatloo, B.; Teodorescu, R. Fractional-Order Control Techniques for Renewable Energy and Energy-Storage-Integrated Power Systems: A Review. *Fractal Fract.* **2023**, *7*, 391. [CrossRef]
51. Chen, M.; Ge, S.S. Adaptive Neural Output Feedback Control of Uncertain Nonlinear Systems with Unknown Hysteresis Using Disturbance Observer. *IEEE Trans. Ind. Electron.* **2015**, *62*, 7706–7716. [CrossRef]
52. Mani, P.; Rajan, R.; Shanmugam, L.; Joo, Y.H. Adaptive Fractional Fuzzy Integral Sliding Mode Control for PMSM Model. *IEEE Trans. Fuzzy Syst.* **2019**, *27*, 1674–1686. [CrossRef]
53. Wang, C.; Liang, M.; Chai, Y. Adaptive neural network control of a class of fractional order uncertain nonlinear MIMO systems with input constraints. *Complexity* **2019**, *2019*, 1410278. [CrossRef]